© 2019. Published by The Company of Biologists Ltd | Development (2019) 146, dev170837. doi:10.1242/dev.170837

RESEARCH ARTICLE

Regulation of Notch signaling by the chromatin-modeling protein Hat-trick

Ankita Singh, Maimuna S. Paul, Debdeep Dutta, Mousumi Mutsuddi* and Ashim Mukherjee*

ABSTRACT

Notch signaling plays a pleiotropic role in a variety of cellular processes, including cell fate determination, differentiation, proliferation and apoptosis. The increasingly complex regulatory mechanisms of Notch signaling account for the many functions of Notch during development. Using a yeast two-hybrid screen, we identified the *Drosophila* DNA-binding protein Hat-trick (Htk) to be an interacting partner of Notch-intracellular domain (Notch-ICD); their physical interaction was further validated by co-immunoprecipitation experiments. *htk* genetically interacts with Notch pathway components in trans-heterozygous combinations. Loss of *htk* function in *htk* mutant somatic clones resulted in the downregulation of Notch targets, whereas its overexpression caused ectopic expression of Notch targets, without affecting the level of the Notch protein. In the present study, immunocytochemical analyses demonstrate that Htk and overexpressed Notch-ICD colocalize in the same nuclear compartment. Here, we also show that Htk cooperates with Notch-ICD and Suppressor of Hairless to form an activation complex and binds to the regulatory sequences of Notch downstream targets such as Enhancer of Split complex genes, to direct their expression. Together, our results suggest a novel mode of regulation of Notch signaling by the chromatin-modeling protein Htk.

KEY WORDS: Cell signaling, Notch, Activation complex, Enhancer of Split complex, Chromo-domain, *Hat-trick*, *Drosophila*

INTRODUCTION

Notch signaling is an evolutionarily conserved pathway that regulates a variety of developmental processes, including acquisition of specific cell fates, cell proliferation, differentiation, self-renewal and cell death programs (Cabrera, 1990; Egan et al., 1998; Artavanis-Tsakonas et al., 1999; Fehon et al., 2007; Fortini, 2009; Liu et al., 2010; Andersson et al., 2011; Guruharsha et al., 2012). Notch is subjected to tight regulation at the level of receptor and ligand biosynthesis, post-translational modifications, ligand–receptor interaction and trafficking. The intricate regulatory mechanisms of Notch signaling account for the diverse functions of same pathway in numerous cellular contexts during organism development (Baron et al., 2002). The Notch receptor is synthesized as a 300 kDa single polypeptide precursor that is cleaved by furin-like convertase(s) during maturation in the trans-Golgi network. The N-terminal extracellular subunit and a C-terminal transmembrane intracellular subunit join via a noncovalent bond to form a single transmembrane heterodimeric receptor that translocates to the cell membrane (Blaumueller et al., 1997; Logeat et al., 1998). Notch signal transduction is initiated when the Notch receptor interacts with its ligands, Delta and Serrate (*Drosophila*), from neighboring cells (Rebay et al., 1991), and initiates proteolytic cleavage by the A Disintegrin And Metalloprotease domain (ADAM)/TNFα Converting Enzyme (TACE)/Kuzbanian family of metalloproteases (Brou et al., 2000; Mumm et al., 2000). This cleavage of the extracellular domain from the transmembrane domain generates a membrane-tethered Notch, known as Notch extracellular truncation (NEXT) fragment, that is subsequently cleaved by the γ-secretase complex (De Strooper et al., 1999; Struhl and Greenwald, 1999; Ye et al., 1999). This cleavage results in the release of Notch-intracellular domain (Notch-ICD/NICD), which eventually translocates to the nucleus via Importin-α3 (Sachan et al., 2013). In the nucleus, Notch-ICD binds to, and activates, the transcription factor, Suppressor of Hairless [Su(H)] in *Drosophila* (CBF1/RBPJ in vertebrates) and displaces the co-repressors and recruits co-activators, including Mastermind (Mam), leading to the activation of Notch target genes (Fortini and Artavanis-Tsakonas, 1994; Struhl and Adachi, 1998; Wu et al., 2000; Cau and Blader, 2009). In *Drosophila*, most of the Notch target genes identified so far are in the Enhancer of Split complex [E(spl)]. This is a complex locus containing, among others, seven transcription units (*mδ*, *m7*, *m5*, *m3*, *mβ*, *mγ* and *mδ*), which encode basic helix-loop-helix (bHLH) transcriptional repressors (Delidakis and Artavanis-Tsakonas, 1992; de Celis et al., 1996; Bray and Furriols, 2001). This complex of genes is often regulated by Notch signaling and is important for neurogenesis and cell fate decisions.

To identify novel regulators of Notch-ICD, a yeast two-hybrid screen was performed, which identified *Drosophila* Hat-trick (Htk) as an interacting partner of Notch-ICD. Htk is a DNA-binding protein that harbors the AT-rich interacting domain (ARID), chromatin organization modifier (Chromo) and Tudor domains (Fig. 1A). These domains are present in proteins that are involved in DNA binding and chromatin modeling (Herrscher et al., 1995; Iwahara, and Clubb, 1999; Akhtar et al., 2000; Brehm et al., 2000; Bouazoune et al., 2002; Iwahara et al., 2002; Kim et al., 2006). In addition to the sequence homology with chromatin-remodeling proteins, Htk is also reported to interact with the histone deacetylase, Sin3A (Spain et al., 2010). We recently revealed its role in mediating important chromatin functions during *Drosophila* oogenesis, such as karyosome structure and double-strand break (DSB) repair (Singh et al., 2018). Htk is presumed to be a chromatin-modeling protein, although its functional characterization is incomplete. Its name derives from its putative role in heterochromatinization and its influence on TDP-43-mediated toxicity (Sreedharan et al., 2015). The *htk* gene encodes two annotated transcript variants that are translated into two polypeptides of 186 kDa and 259 kDa, respectively. Bioinformatic analysis revealed that Htk can regulate transcription from the RNA

Department of Molecular and Human Genetics, Institute of Science, Banaras Hindu University, Varanasi 221005, Uttar Pradesh, India.

*Authors for correspondence (ashim04@gmail.com; mousumi_mutsuddi@yahoo.com)

A.S., 0000-0002-6045-1757; M.S.P., 0000-0002-1864-4707; D.D., 0000-0003-0989-7013; M.M., 0000-0002-1339-8535; A.M., 0000-0002-3523-7089

Received 11 August 2018; Accepted 16 May 2019

Development (2019) 146, dev170837. doi:10.1242/dev.170837

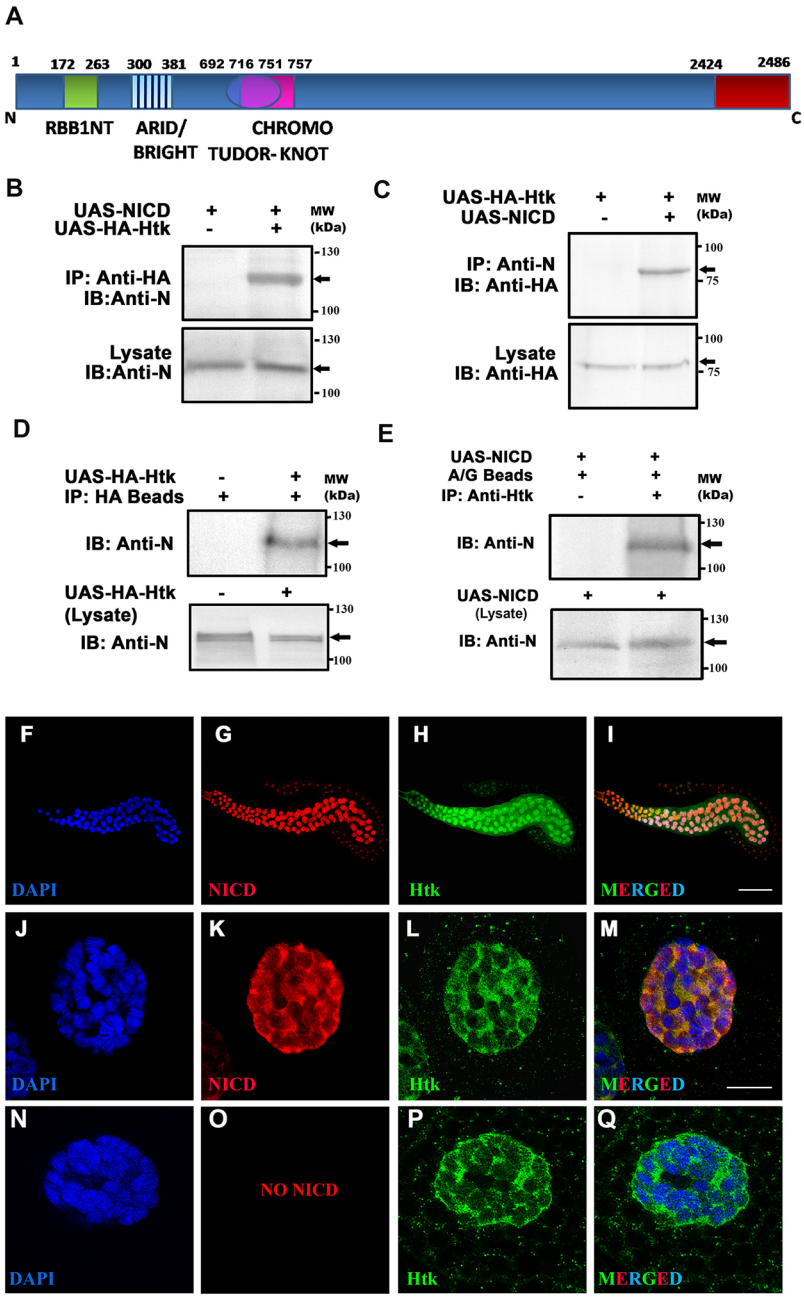

Fig. 1. *Drosophila* Notch binds with Htk. (A) Schematic of the Htk protein and its conserved domains. A specific region of Htk at the C terminus (amino acids 2424-2486, red) was used for antibody generation. (B-C) Co-immunoprecipitation was carried out with wing disc lysates overexpressing HA-Htk and Notch-ICD using *vg-GAL4*. (B) HA-Htk immunoprecipitated Notch-ICD, which was detected by anti-Notch antibodies (C17.9C6). (C) Notch-ICD also immunoprecipitated HA-Htk, which was detected by anti-HA antibodies. (D) A protein lysate was made from tissue overexpressing HA-Htk alone, and from wild-type tissue (only endogenous Htk); HA-Htk co-immunoprecipitated endogenous Notch. No Notch protein bands were observed in the negative control. (E) Co-immunoprecipitation was carried out using anti-Htk antibodies with larval salivary gland lysates in which Notch-ICD was overexpressed by *sgs-GAL4*. Endogenous Htk was sufficient to immunoprecipitate expressed Notch-ICD, which that was detected by anti-Notch antibodies. The lower blot in each experiment shows the presence of the specified protein in both the experimental and control lysates. The plus symbol indicates the presence and the minus symbol indicates the absence of the specified reagent in B-D. (F-M) Htk colocalized with expressed Notch in the cell nucleus. Notch-ICD was expressed under the control of *sgs-GAL4* and was stained with anti-Notch antibodies (red; G, K). DAPI marks the chromatin (blue; F,J,N). Anti-Htk antibodies were used to stain endogenous Htk protein (green; H,L,P). The second row is higher magnification images of a single cell from a larval salivary gland from the first row. (I,M) Merged images show that Htk and Notch colocalized in the cell nucleus (I), within chromatin and interchromatin spaces (M). (N-Q) The third row is the higher magnification images of a single cell from a larval salivary gland showing the expression of endogenous Htk without Notch-ICD overexpression. Notch-ICD overexpression did not cause any significant change in the expression and localization of endogenous Htk (L,P). Images in I, M and Q are merges of those in F-H, J-L and N-P, respectively. Scale bars: 200 µM in F-I and 20 µM in J-Q. RBBNT, retinoblastoma binding protein 1 N-terminal domain.

polymerase II promoter (Gaudet et al., 2010). The mammalian orthologs of Htk, ARID4A and ARID4B, are members of the chromatin-remodeling complex and function as transcriptional repressors upon recruitment by tumor suppressor RB; thus, they are also known as RB-Binding Protein 1 (RBBP1) and RBBP1-Like Protein 1 (RBBP1L1), respectively (Defeo-Jones et al., 1991; Lai et al., 1999, 2001; Cao et al., 2001; Fleischer et al., 2003).

In the present study, we characterized the functional significance of the Notch–Htk interaction, hypothesizing that Htk is a part of the Notch-Su(H) activation complex. Using molecular and genetic analyses, we found that Htk acts as a positive regulator of Notch signaling by physically interacting with Notch-ICD, a result confirmed by co-immunoprecipitation experiments. *htk* also showed genetic interactions with components of the Notch signaling pathway. Loss- and gain-of-function studies revealed its pleiotropic role in regulating various developmental events. Several phenotypes generated by loss or gain of *htk* function mimicked Notch mutant phenotypes, further supporting the role of *htk* as a modulator of Notch signaling. Overexpression of *htk* upregulated Notch signaling, as evidenced by the ectopic expression of the Notch target Cut, without a change in the level of Notch-ICD in developing wing imaginal discs. Conversely, the Notch targets Cut and Wingless were downregulated in *htk* mutant clones, indicating *htk* to be a positive regulator of Notch signaling. Additionally, the Htk protein colocalized with expressed Notch-ICD in the same nuclear compartment. Furthermore, Htk immunoprecipitated Su(H), a transcription factor involved in Notch signaling. Fragments of the regulatory sequences of E(spl) complex genes, which are Notch targets, were chromatin immunoprecipitated with Htk, confirming Htk as a component of the regulatory complex. Real-time analysis of E(spl) complex gene expression from *htk* overexpressed tissue confirmed Htk as part of the activation complex. Thus, our functional analyses indicate Htk to be a novel modulator of Notch signaling in *Drosophila*.

Development (2019) 146, dev170837. doi:10.1242/dev.170837

RESULTS

Htk is an interacting partner of Notch

In a yeast two-hybrid screen, we identified Htk as an interacting partner of Notch. In the same screen, multiple positive clones of Su(H), a well-established binding partner of Notch-ICD, were also identified, which validated our approach. The amino terminus of Notch-ICD (amino acids 1765-1895) was used as a bait to screen 6×10^6 cDNAs from a *Drosophila* 0-24 h embryonic library. Eleven positive clones (His^+) were isolated and found to encode overlapping *htk* cDNAs. Sequence analysis of overlapping domains revealed that the C terminus of Htk (amino acids 2424-2486), which is specific to the protein, was sufficient for binding to Notch-ICD (Fig. S1A).

Co-immunoprecipitation experiments further validated the physical interaction of Notch with Htk. Using extracts from wing discs coexpressing hemagglutinin (HA)-tagged Htk and Notch-ICD, we demonstrated that Htk or Notch could be co-immunoprecipitated with either anti-HA or anti-Notch antibodies (Fig. 1B,C). Moreover, expressed HA-Htk was able to co-immunoprecipitate endogenous Notch (Fig. 1D). Endogenous Htk was also sufficient to immunoprecipitate Notch from larval salivary glands when only Notch-ICD was overexpressed (Fig. 1E).

Immunocytochemical analysis revealed that endogenous Htk (marked by an anti-Htk antibody, generated previously; Singh et al., 2018) and overexpressed Notch-ICD colocalized in the same nuclear compartment (Fig. 1F-Q).

htk genetically interacts with Notch pathway components

To further analyze the functional implications of the physical interaction between the Htk and Notch proteins, we investigated whether mutations in *htk* and *Notch* pathway components displayed genetic interactions in trans-heterozygous combinations. Three *htk* loss-of-function alleles, htk^{71}, htk^{49} and htk^{37}, were used for genetic interaction studies. Both *Notch* and *htk* are located on I chromosome and their null alleles are hemizygous lethal; therefore, it was not possible to check the genetic interaction between them under trans-heterozygous conditions. A trans-heterozygous combination of a *htk* allele and a dominant negative allele of *Notch* (*UAS-Notch-DN*) enhanced the wing-nicking phenotype, indicating a further decrease in Notch function (Fig. 2A-D). An enhanced wing-nicking phenotype also occurred when different *htk* alleles combined with the *Su(H)* gain-of-function allele, *Su(H)T4* (Fig. 2E-H, Fig. S1B) and loss-of-function allele, *Su(H)1* (Fig. 2I-L, Fig. S1B). Su(H) is a DNA-binding protein component of the Notch signaling pathway; its gain- or loss-of-function should result in reduced Notch signaling activity, as it is a component of both the repression and activation complexes (Furriols and Bray, 2000). Excess Su(H) competes with the normal Su(H) and Notch-ICD-containing activation complex, and free Su(H) alone can

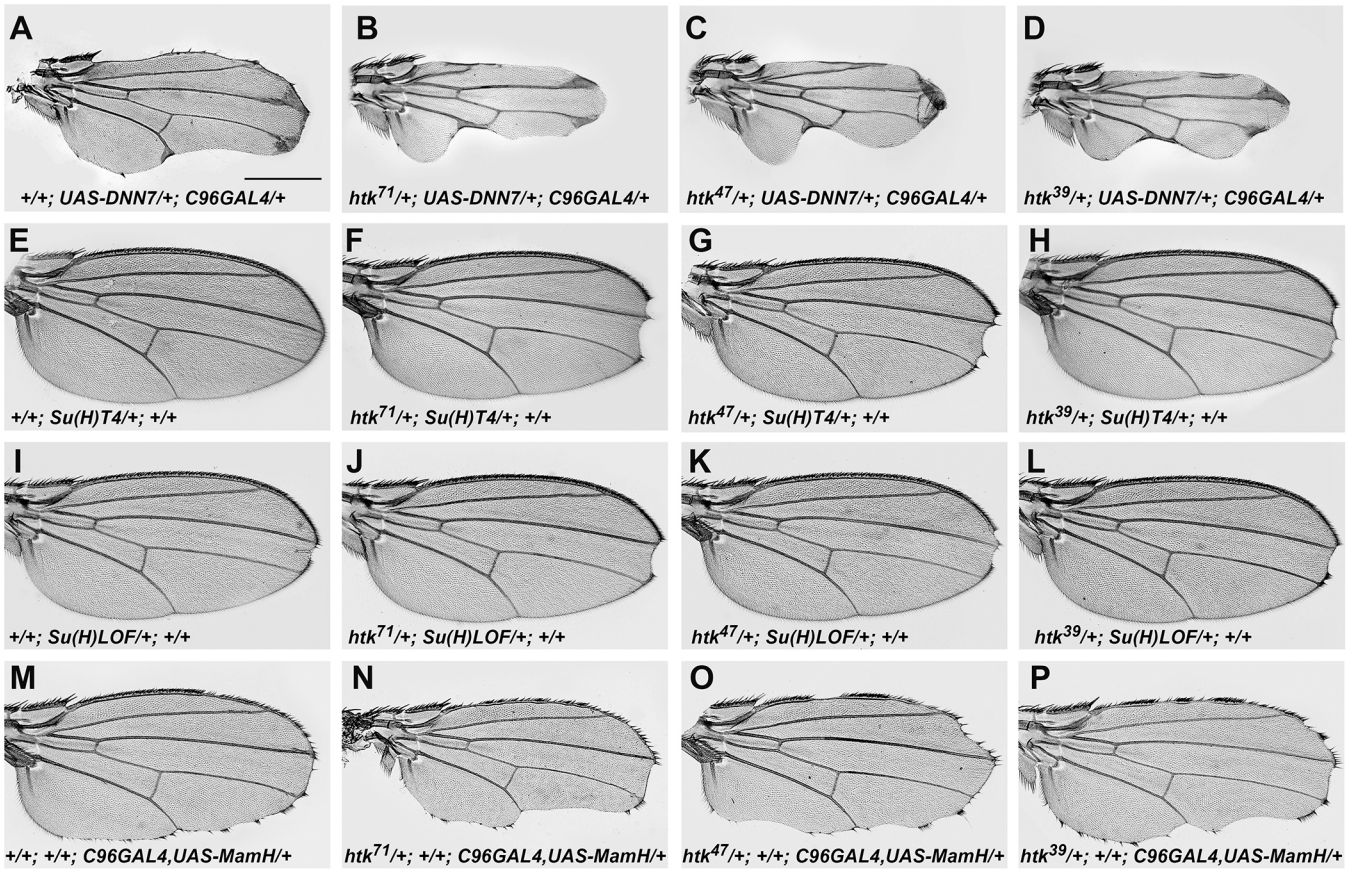

Fig. 2. Genetic interactions of *htk* with Notch pathway components. Representative wings from different Notch pathway component mutants are shown in the first column and those in trans-heterozygous combination with the *htk* mutants htk^{71}, htk^{47} and htk^{39} are shown in the second, third and fourth columns, respectively. (A-D) Dominant negative Notch driven at the wing margin using *C96-GAL4* caused a wing-notching phenotype (A), which was enhanced in trans-heterozygous combination with different *htk* alleles and the wings appeared shorter (B-D). (E-L) Similarly, when the *Su(H)* gain-of-function allele *Su(H)T4* (E) and loss-of-function allele *Su(H)1* (I) were brought together with different *htk* alleles, the wing-nicking phenotypes increased. (M-P) Serration phenotype of wings expressing dominant negative *Mam* using *C96-GAL4* (M) was enhanced in combination with *htk* alleles. *n*=100 wings for each genotype. The penetrance of the phenotype for each genotype was 100% except for *Su(H)T4* heterozygotes with *htk* alleles, in which penetrance of the phenotype was 85%. Scale bar: 500 µm.

Development (2019) 146, dev170837. doi:10.1242/dev.170837

bind to DNA, inactivating those downstream Notch target genes that require both Su(H) and Notch-ICD for their activation (Furriols and Bray, 2000). Thus, we hypothesize that, similar to the case of the Su(H) loss-of-function allele, when we reduced the dose of *htk* along with the heterozygous Su(H) gain-of-function allele, there was a further reduction of Notch signaling, as shown by the increased wing-nicking phenotype in both cases. *C96-GAL4*-driven expression of dominant negative C-terminal Mam truncation displays a fully penetrant wing-nicking phenotype (Fig. 2M) (Helms et al., 1999; Kankel et al., 2007). Reducing the dose of *htk* in these individuals elicited an enhanced wing-notching phenotype (Fig. 2M-P). Our genetic interaction screen revealed that, when combined with Notch pathway mutants, different *htk* loss-of-function mutants further reduced the Notch signaling activity, resulting in more severe phenotypes. We note that *htk* mutants showed a strong genetic interaction with the transcription factors and co-activators involved in the Notch signaling pathway.

htk loss of function results in downregulation of Notch signaling without any alteration of Notch protein levels

We generated *htk* mutant somatic clones in larval wing imaginal discs using different *htk* loss-of-function mutant alleles and the FLP-FRT system (Xu and Rubin, 1993). In htk^{71} mutant clones, no significant change in the Notch protein level was observed compared with the surrounding wild-type cells (Fig. 3A-A‴). We also checked the status of Notch signaling activity by investigating the expression level of downstream targets of Notch, Cut and Wingless. Notch induces Cut and wingless expression at the dorsoventral (DV) boundary of the developing wing disc (Neumann and Cohen, 1996). In the current study, protein levels of both Cut and Wingless were significantly reduced in htk^{71} mutant clones compared with wild-type sister cells at the DV boundary (Fig. 3B-D‴). In addition, expression of a Notch signaling reporter, Notch responsive element Green Fluorescent Protein (NRE-GFP), was significantly reduced in *htk* loss-of-function clones (Fig. 3E-E‴). Adults carrying *htk* clones displayed Notch loss-of-function phenotypes, such as wing notching and increased scutellar bristle phenotypes (Fig. S5G,H). Thus, loss of Htk resulted in reduced Notch signaling activity without affecting the level of the Notch receptor.

Overexpression of Htk modulates Notch signaling activity

We further examined the influence of ectopic expression of *htk* on Notch expression and its localization. HA-tagged *htk* was overexpressed in the anterior-posterior (AP) margin of the wing disc using the *ptc-GAL4* driver; however, expression of HA-Htk did not affect the level or localization of the endogenous Notch protein (Fig. 4A-C). We then investigated the level of Notch signaling activity by checking the status of Cut, which expresses under the influence of Notch signaling at the DV boundary of the wing disc (Neumann and Cohen, 1996). Overexpression of *HA-htk* at the AP boundary of the wing discs resulted in ectopic expression of Cut along the AP junction of the pouch region within the wing disc (Fig. 4D-I).

Loss- and gain-of-function of *htk* results in wing and eye phenotypes similar to those in Notch mutants

Using tissue-specific GAL4 drivers (Brand and Perrimon, 1993), we also observed the downregulatory and gain-of-function effects of *htk* in adult tissues, as also seen in imaginal discs (Fig. S1C,D). *htk-*

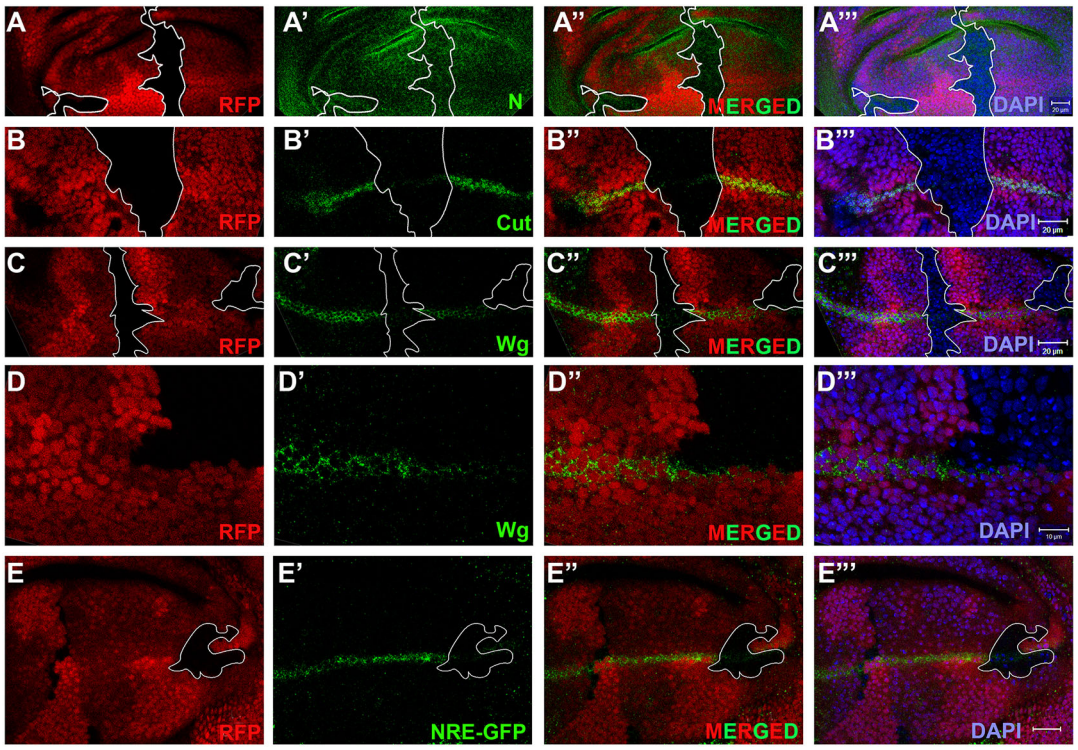

Fig. 3. Loss-of-function clones of *htk* display reduced Notch signaling activity without significantly affecting its endogenous localization or expression. (A-E‴) Loss-of-function clones of *htk* using the htk^{71} allele were generated with the FLP/FRT system; htk^{71} clones were marked by the absence of Red Fluorescent Protein (RFP) expression. (A-C‴, E-E‴) are lower magnification and D-D‴ are higher magnification images. Notch staining in wing discs of such clones displayed no significant change in the localization and expression of endogenous Notch (A′), whereas the expression of the Notch downstream targets, Cut (B′) and Wingless (C′, D′), and of a Notch signaling reporter line, NRE-GFP (E′), was significantly reduced in *htk* loss-of-function clones. Third-column images are merges of those in the first and second columns. The fourth column shows merged images with DAPI staining in discs that showed nuclei integrity. The outline borders the *htk* null clones. Scale bars: 20 µm in A-C‴, E-E‴ and 10 µm in D-D‴.

Development (2019) 146, dev170837. doi:10.1242/dev.170837

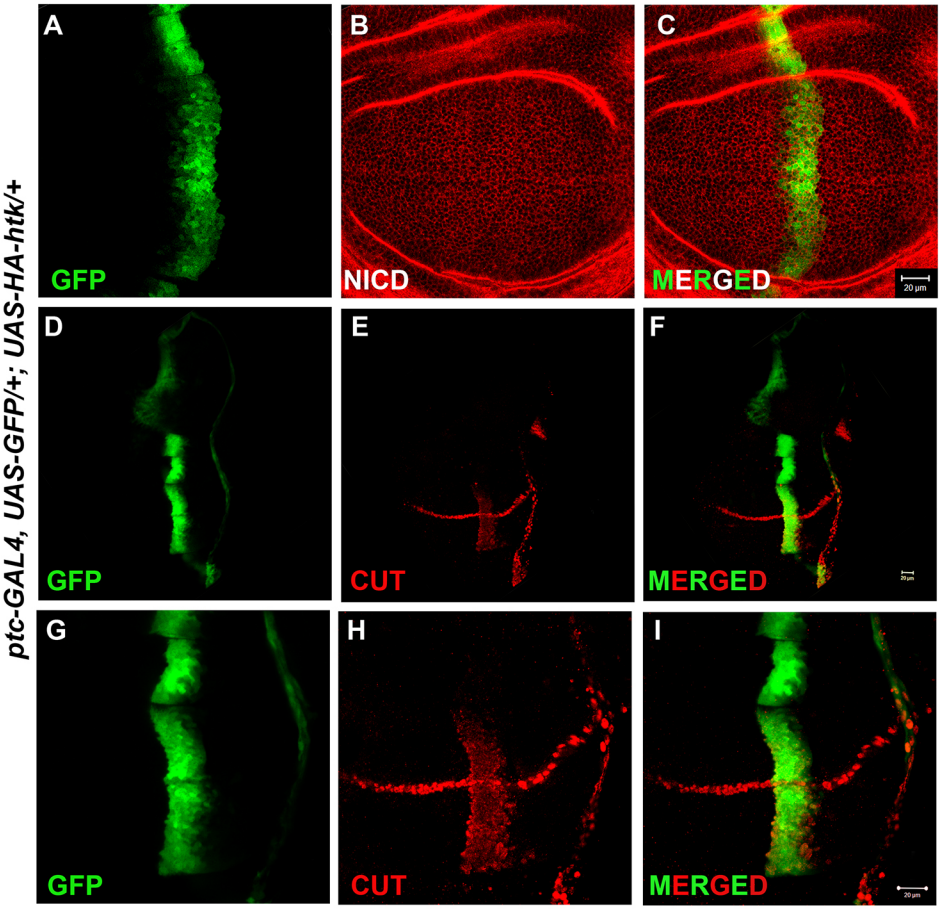

Fig. 4. Effect of overexpression of *htk* on Notch expression and its signaling activity at the junction of the AP-DV boundary in the wing disc. (A-C) *patched-GAL4*-driven expression of HA-Htk at the AP boundary in the wing disc (marked with GFP) (first column) resulted in no change in Notch (in red) expression. (D-F) Ectopic expression of Notch target, Cut, at the AP boundary is clearly visible in the pouch region of wing disc. (G-I) Higher magnification images of D-F, respectively. Scale bars: 20 µm.

RNAi was used to investigate the tissue-specific loss-of-function effects of *htk*. However, this RNAi stock caused weak RNA interference and, as a result, variability in expressivity and incomplete penetrance were observed. Downregulation of *htk* using *apterous-GAL4* in the dorsal region of wing discs, which form the adult thorax and wing, resulted in increased scutellar bristles in comparison with wild type (Fig. S2C,D) and wings that were bent out and upwards, probably because of thorax muscle defects (Fig. S2A,B). These wings also had extra rows of bristles (Fig. S2G). Downregulation of *htk* using the *patched-GAL4* driver in the AP boundary reduced the intervein distance between the L3 and L4 veins and also reduced the first cross-vein (Fig. S2F). *dpp-GAL4*-driven downregulation of *htk* also resulted in extra vein material and, occasionally, an extra cross-vein at the AP boundary (Fig. S2I). Furthermore, loss of *htk* at the wing margin using *C96-GAL4* resulted in extra vein material, and areas with thinner cuticle at, or near, the wing margin (Fig. S2J). *MS1096-GAL4*-driven *htk-RNAi* also resulted in similar phenotypes (data not shown). *engrailed-GAL4*-driven *htk-RNAi* resulted in thinner wing blades in the posterior region of the wings (Fig. S2K). Thus, loss of *htk* in different regions of wings resulted in extra vein material, extra bristles and small patches of disorganized tissue (Fig. S2H-H″). Loss of *htk* in the eye using *eyeless-GAL4* resulted in loss of ommatidia and reduced eye size (Fig. S2L). Most of these *htk*-downregulated phenotypes also corresponded to Notch loss-of-function phenotypes. It is well established that Notch is needed for wing margin, vein and sensory bristle development, and its loss also results in reduced intervein distance and eye size (Hartenstein and Posakony, 1990; Go and Artavanis-Tsakonas, 1998; Casso et al., 2010).

Additionally, using various tissue-specific GAL4 drivers, HA-tagged *htk* was overexpressed in different regions of the wing discs and eye discs. Gain of function of HA-Htk in the dorsal region of wing discs, using an *apterous-GAL4* driver, resulted in the loss of scutellar bristles, reduced scutellum size and severe wing blisters (Fig. S3B-D). Overexpression in the posterior region of wing discs using *engrailed-GAL4* resulted in bending of the third wing vein, a thinner wing blade and an incomplete fifth vein (Fig. S3H). *HA-htk* gain of function in the eye using *GMR-GAL4* and *eyeless-GAL4* drivers resulted in eye roughening (Fig. S3J,L) and loss of ommatidia (Fig. S3F), respectively. A few of these observed phenotypes were similar to Notch gain-of-function phenotypes, such as the loss of bristles and vein material and an increase in eye roughening (Hartenstein and Posakony, 1990; Go and Artavanis-Tsakonas, 1998; Casso et al., 2010).

htk shows epistatic interaction with *Notch* and *Su(H)* and is required for Notch-Su(H)-mediated downstream target gene expression

To determine the epistatic interaction of *htk* with *Notch* or *Su(H)*, we examined whether *htk* could rescue loss- or gain-of-function phenotypes of *Notch* or *Su(H)*. A severe wing notching phenotype was caused by a reduction in Notch signaling when *Notch-RNAi* (*NIRM*) was expressed at the wing margin (Fig. S4A). The wing-nicking phenotype was significantly rescued when HA-tagged *htk* was overexpressed in this background (Fig. S4B). By contrast, overexpression of *Notch-ICD* or *Su(H)VP16* at the wing margin driven by *C96-GAL4* resulted in irregular wing margin bristles (Fig. S4C-E). This phenotype was significantly rescued by

Development (2019) 146, dev170837. doi:10.1242/dev.170837

decreasing the expression of *htk* using *htk-RNAi* in the same background (Fig. S4H-J,V-W). Thus, overexpression of *htk* can rescue the wing phenotypes caused by *Notch* loss of function, and a reduction in *htk* expression leads to rescue of the gain-of-function effects of *Notch* and *Su(H)VP16* in the wing margin (Fig. S4A-J,V-W).

Additionally, when *HA-htk* was coexpressed with *Notch-ICD* or *Su(H)VP16* at the wing margin using a *C96-GAL4* driver, there was an increase in the wing margin irregularities, reflecting the synergistic behavior of *htk* with *Notch* and *Su(H)VP16* (Fig. S4M-O).

We further confirmed this epistatic interaction by looking at the expression of the Notch downstream target, Cut (Neumann and Cohen, 1996). Loss of Cut expression was observed when *Notch-RNAi* was expressed at the DV boundary of the wing disc using a *C96-GAL4* driver (Fig. S4Q). The reduced activity of Notch signaling, as indicated by the reduction in Cut expression, was partially rescued when *HA-htk* was expressed in the same background (Fig. S4R,X). By contrast, reducing the expression of *htk* using *htk-RNAi* partially rescued the ectopic Cut expression caused by overexpression of *Su(H)VP16* at the DV boundary of wing disc using the *C96-GAL4* line (Fig. S4T-U,Y).

To further confirm the role of Htk in Notch-Su(H)-mediated downstream target gene expression, we overexpressed *Notch-ICD* or *Su(H)VP16* in *htk* mutant clonal cells using the MARCM technique (Lee and Luo, 2001). In *UAS-Notch-ICD* and *UAS-Su(H)VP16* lines, *Notch-ICD* and *Su(H)VP16* were under the *UAS* promoter and *tub-GAL4* was used to drive *Notch-ICD* and *Su(H)VP16* globally; however, the presence of *GAL80* inhibited *GAL4*-induced expression of *Notch-ICD* and *UAS-Su(H)*VP16 in all cells except those in which *GAL80* was eliminated because of FLP-FRT-mediated somatic recombination events. In the same mutant clonal cells, *htk* gene function was also eliminated. As a result, these *Notch-ICD* and *Su(H)*VP16-overexpressing clonal cells, which were also marked with GFP, were for mutated the *htk* gene. MARCM analysis of wild-type clones without *htk* mutation was also carried out. The status of the Notch downstream target, Cut, was examined in the clonal cells. Without the *htk* mutation, *Notch-ICD* and *Su(H)VP16*-expressing clones showed ectopic Cut expression (Fig. 5A-D,I-L). Interestingly, in the absence of *htk*, *Notch-ICD* and *Su(H)VP16* were unable to show the complete activity of Notch, and a reduction in ectopic Cut expression was observed (Fig. 5E-H,M-P).

In addition to MARCM analysis, *Su(H)VP16* was overexpressed at the DV boundary using a C96-*GAL4* driver; in this background, FLP-FRT-mediated *htk* null clones were generated. Many of these *htk* null clones also showed similar results displaying reduction of ectopic Cut expression (Fig. 5Q-T). Thus, together these results confirmed that *htk* is required for complete Notch signaling activity, and *NICD* or *Su(H)* cannot execute all the functions of Notch in the absence of *htk*.

Htk is a component of the Notch activation complex

Immunocytochemical analysis revealed that endogenous Htk and overexpressed Notch-ICD colocalized in the same nuclear compartment (Fig. 1F-I). These two proteins overlapped in the interchromatin and chromatin space within the nucleus (Fig. 1J-M). In the nucleus, Notch forms an activation complex to express downstream target genes (Fortini and Artavanis-Tsakonas, 1994; Struhl and Adachi, 1998; Borggrefe and Oswald, 2016). Thus, we investigated whether Htk is a component of the Notch-ICD activation complex in the nucleus. If it is, Htk should co-immunoprecipitate Su(H), a component of the Notch-ICD activation complex. Co-immunoprecipitation experiments with HA-tagged Htk revealed that HA-Htk was able to pull down endogenous Su(H) when Htk and Notch-ICD were coexpressed in larval wing discs (Fig. 6A). Additionally, HA-Htk was sufficient to immunoprecipitate endogenous Su(H) when only endogenous Notch was present (Fig. 6A). This confirmed that Htk and Su(H) belong to the same activation complex. Given that Htk physically interacted with Notch-ICD (Fig. 1), we concluded that Htk is a component of the Notch-Su(H) transcription complex.

We also explored the mechanism of regulation of Notch signaling by *htk*. The nuclear localization, DNA-binding ability and physical interaction of Htk with Notch-ICD prompted us to hypothesize that Htk binds to the promoter sequences of Notch targets and cooperates with Notch-ICD for activation of these downstream targets. We performed chromatin immunoprecipitation (ChIP) of expressed HA-tagged Htk using HA beads followed by PCR using primers (Fig. S5J) for promoter sequences of the well-established Notch targets, E(spl) complex genes. ChIP experiments can identify the *in vivo* association of transcription factors with regulatory elements. We observed that Htk binds to the promoter sequences of Notch target genes (Fig. 6B). To further confirm that Htk is a component of the activation complex and not the repressor complex, we observed the status of two of these E(spl) complex genes, *E(spl)m8* and *E(spl)mβ*, in *htk* loss-of-function clones. *LacZ* reporter stocks were used to verify their expression, which was downregulated in *htk* loss-of-function clones (Fig. S5A-F). Furthermore, real-time analysis showed that the expression of E(spl) complex genes increased with the increase in Htk expression (Fig. 6C), confirming our hypothesis that Htk is an important component of the Notch co-activation complex. Thus, we showed that Htk interacts with the Notch-ICD and is recruited to promoters of Notch target genes to activate their expression (Fig. 6D).

DISCUSSION

The Notch signaling pathway regulates a variety of cellular processes. Despite the plethora of information about this conserved signaling pathway, the intricate regulatory mechanism of Notch activation is far from complete. Here, we report for the first time that the chromatin-modeling protein Htk is a novel interactor of Notch-ICD. Htk is a Chromo, ARID and Tudor domain-containing protein, and these domains render this protein with putative DNA-binding activity. Htk was identified as an interacting partner of Notch-ICD in a yeast two-hybrid screen; Htk was found to physically interact with Notch-ICD and to interact genetically with mutants of Notch pathway components, especially those of the transcription factor complex. Htk is a nuclear protein that colocalizes with expressed Notch-ICD inside the nucleus. Our loss-of-function and the complementary gain-of-function analyses indicated that Htk is involved in the regulation of Notch signaling. We also showed that Htk is a component of the Notch activation complex. In the absence of Notch signaling, CSL [CBF-1/RBPJ in vertebrates, Su(H) in *Drosophila melanogaster*, and lag-1 in *Caenorhabditis elegans*] remains associated with the repressor complex and actively represses the transcription of target genes. Upon activation of Notch signaling, CSL binds to Notch-ICD, displaces the CSL-associated repressor complex and recruits co-activators, leading to the transcriptional activation of Notch target genes (Fortini and Artavanis-Tsakonas, 1994; Struhl and Adachi, 1998). It has been predicted that CSL-mediated transcription of downstream target genes is switched on or off depending on the molecular signature on the chromatin created by associated activator or repressor complexes, respectively (Borggrefe and Oswald, 2016; Giaimoa et al., 2017). Surprisingly the DNA-binding affinity of

Development (2019) 146, dev170837. doi:10.1242/dev.170837

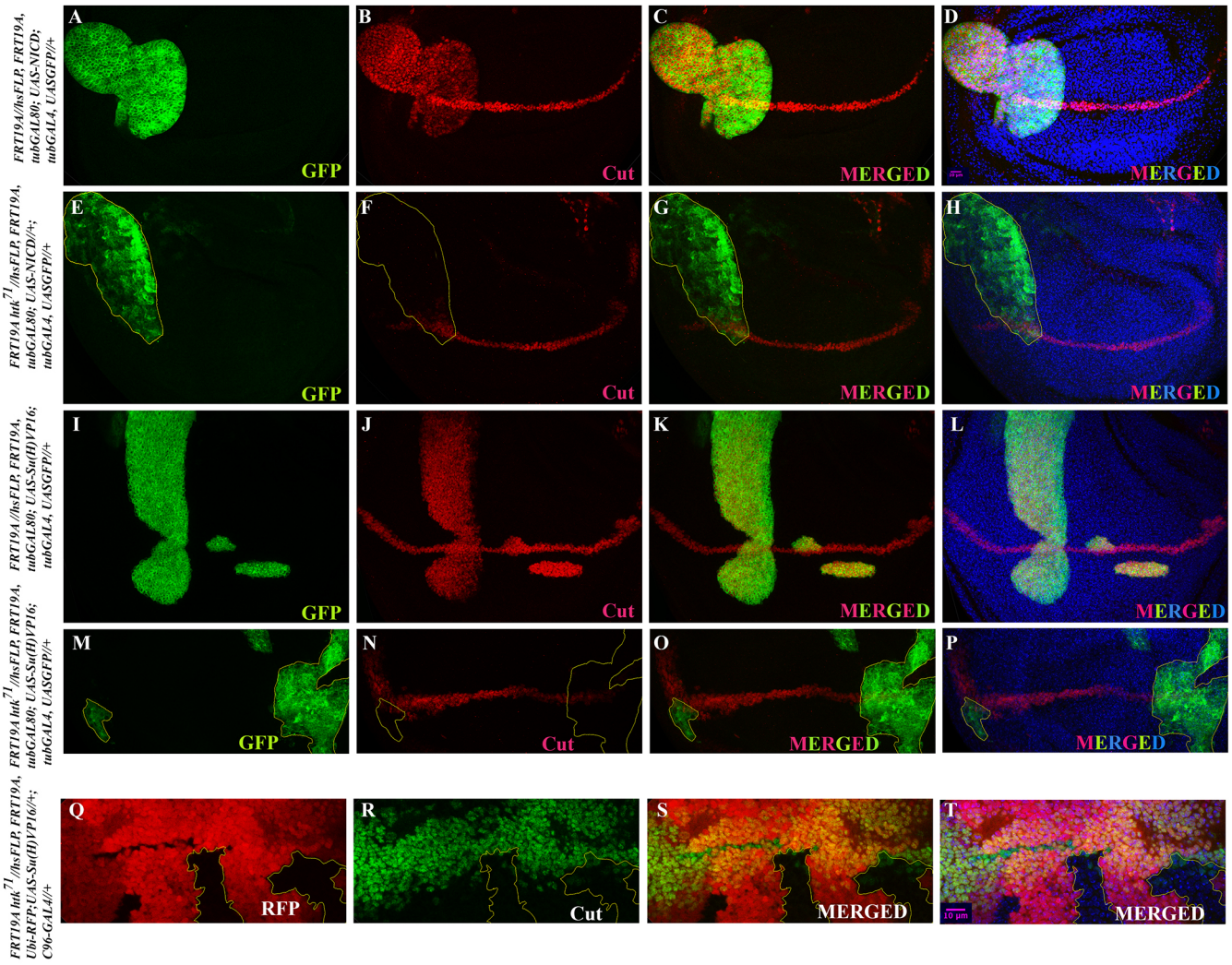

Fig. 5. *htk* is required for complete Notch signaling activity. (A-P) MARCM analysis to show epistatic interaction of *htk* with *Notch* and *Su(H)*. GFP-stained MARCM-derived clones were generated in wing imaginal discs. Images in the first column represent the clonal area, and those in the second column show the expression of the Notch downstream target, Cut. Images in the third and fourth column are merged images of the first and second column, and stained with DAPI, respectively. Cut expression was checked in MARCM-derived *NICD* (E-H) or *Su(H)VP16* (M-P)-overexpressing htk^{71}mutant clones and wild-type (A-D,I-L) clones. (Q-T) *Su(H)VP16* was overexpressed using *C96-GAL4* at the DV boundary and, in this background, *htk* mutant FLP-FRT clones (marked as RFP null) were generated. Ectopic expression of Cut caused by overexpression of *NICD* and *Su(H)VP16* was significantly reduced in the absence of *htk*, which confirmed that NICD and Su(H) could not achieve the full activity of Notch in the absence of Htk. The outline borders the *htk* null clones. Scale bar: 10 µm.

CSL is extremely low. There is no evidence to show that either co-repressor complex binding or Notch-ICD-activator complex binding to CSL has any impact on its DNA-binding affinity. However, it was hypothesized that other DNA-binding proteins in the CSL activator complex might facilitate its chromatin association (Giaimoa et al., 2017). Our results showed that the DNA-binding protein Htk is present in the Su(H) activator complex and leads to the activation of transcription of target genes, such as those in the E(Spl) complex. Epistasis analysis confirmed that Notch-ICD and Su(H) require Htk to execute the complete function of Notch. We hypothesize that the association of Htk in the Notch-ICD-Su(H) activator complex stabilizes and sustains the binding of Su(H) with DNA and, as a result, transcriptional activation of Notch target genes takes place. Thus, our results establish a novel mode of regulation of Notch signaling by the chromatin-modeling protein Htk.

Recent reports revealed that Sin3A physically binds with Htk (Spain et al., 2010) and also with its human homologs ARID4A and ARID4B (Lai et al., 2001; Fleischer et al., 2003; Suryadinata et al., 2011; Wan et al., 2015). The histone deacetylase Sin3A acts as a negative regulator of transcription (Silverstein and Ekwall, 2005; Kadosh and Struhl, 1998). Sin3A is a binding partner of Su(H), and is a part of a transcription repressor complex involved in suppression of Notch target gene expression in the absence of Notch protein (Zhou et al., 2000). However, here we established that Htk is involved in the transcription activation complex to turn on Notch downstream target gene expression in the presence of Notch protein. The exact role of Htk in regulating the switch from repressor to activation complex is yet to be determined. However, we hypothesize that, similar to Su(H), Htk might also be present in both the repressor and activator complexes and might be required to stabilize and sustain the binding of Su(H) to the promoter sequences of Notch downstream target genes in both complexes.

The data presented here revealed Htk to be a positive regulator of the Notch signaling pathway in *Drosophila*. Htk has been previously reported to interact with a repressor protein, such as

Development (2019) 146, dev170837. doi:10.1242/dev.170837

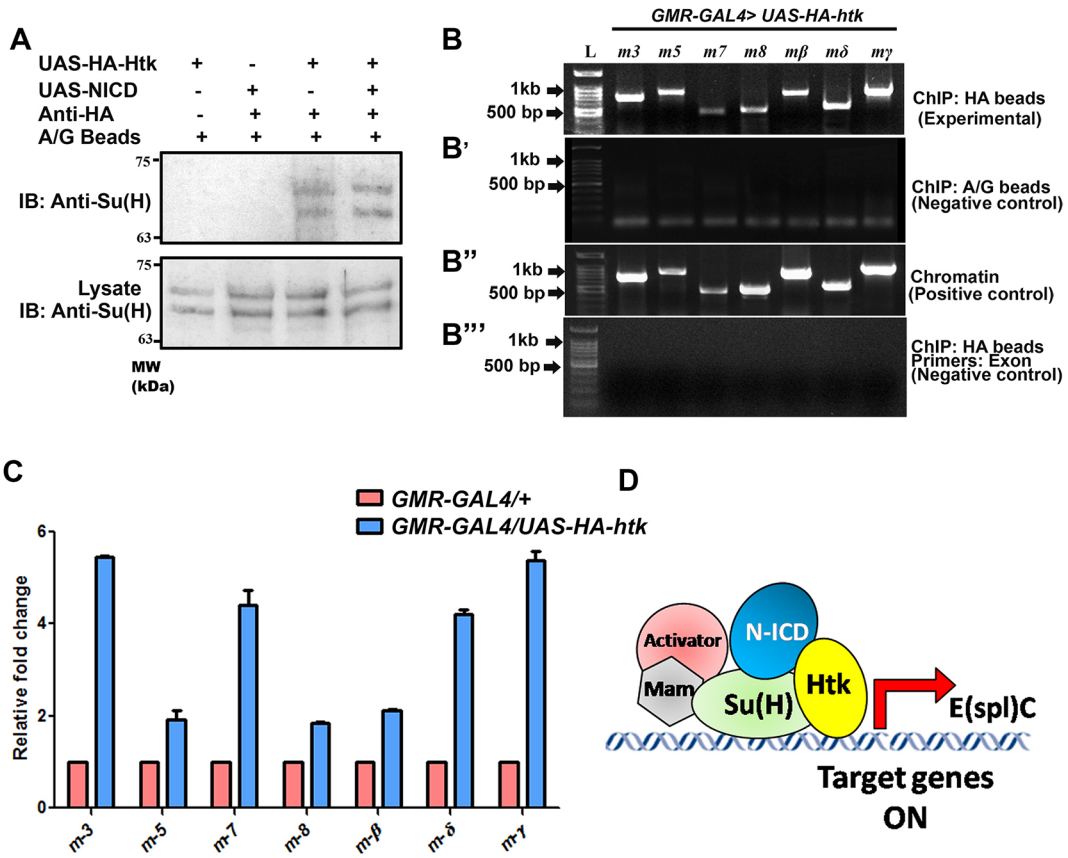

Fig. 6. Htk is a component of the Notch activation complex. (A) A co-immunoprecipitation experiment was performed using lysate prepared from wing discs overexpressing only Notch-ICD, only HA-Htk, and Notch-ICD along with HA-Htk using *vg-GAL4* driver line. Co-immunoprecipitation using lysate overexpressing Notch-ICD and HA-Htk revealed that Htk co-immunoprecipitated endogenous Su(H). Additionally, Htk was sufficient to immunoprecipitate endogenous Su(H) when only endogenous Notch was present. The lower blot shows the presence of Su(H) in both the experimental and control lysates. The plus symbol indicates the presence and the minus symbol the absence of the specified reagent. (B) ChIP was performed using chromatin prepared from adult heads overexpressing HA-Htk driven with *GMR-GAL4*. Immunoprecipitation using HA beads followed by PCR using purified immunoprecipitated DNA as templates and primers specific for regulatory sequences of the Notch direct targets, E(spl) complex genes, showed amplification, confirming that the Htk protein binds to the promoter sequences of the E(spl) complex genes. No amplification was observed in negative controls in which the template DNA used was purified from No-IP chromatin samples (samples without antibody and only A/G beads were added). Chromatin samples before immunoprecipitation contained all the genomic DNA fragments, and were used as positive controls. No amplification was observed in PCR from purified immunoprecipitated DNA using primers specific for exon sequences of E(spl) complex genes, confirming that Htk could specifically bind and immunoprecipitate promoter sequences of E(spl) complex genes. (C) RT-qPCR using cDNA from adult heads with endogenous *htk*, and overexpressed *htk* driven by GMR-GAL4 demonstrated significant upregulation of E(spl) complex genes when *htk* was overexpressed. The experiment was performed in triplicates. Data are mean±s.e.m. (D) A concluding model depicting Htk as a component of the Notch-Su(H) transcription activation complex.

Sin3A (Spain et al., 2010); in addition, the mammalian orthologs of Htk, ARID4A and ARID4B, are members of the chromatin-remodeling complex and function as transcriptional repressors in different contexts (Patsialou et al., 2005). By contrast, we showed that loss of function of Htk decreased Notch signaling, whereas its gain of function upregulated Notch activity, suggesting a transcriptional activator function of Htk in regulating the Notch pathway. This is not the first report showing the positive regulation of Notch signaling by a repressor protein. According to a recent report, a well-established transcriptional repressor protein, the histone deacetylase HDAC1, acts as a positive regulator of Notch signaling (Wang et al., 2018). It has also been shown that HDAC1, along with the HDAC1-associated transcriptional co-repressor Atrophin (Atro), regulates Notch protein levels by promoting Notch transcription (Wang et al., 2018). Similarly, our results also revealed a previously unidentified transcriptional activator function of the predicted repressor complex protein Htk in regulating Notch downstream target gene expression during development.

Similar to CSL in Notch signaling activation, the switch from the repression to activation function of transcription factors was also observed in other signaling pathways, such as T cell factor/lymphoid enhancer factor (TCF/LEF) in the Wnt signaling pathway. Htk might have a similar function in these signaling pathways, although the full spectrum of its function remains to be explored. Given that it is a chromatin-binding protein, Htk could regulate the expression of a range of genes during development. Thus, future studies should explore its function in regulating the activity of different signaling pathways, such as the Wnt, Hippo, Janus kinase (JNK) and Hedgehog (Hh) pathways.

The Notch–Htk interaction might be involved in regulating a spectrum of cellular processes. Recently, it was revealed that loss of *htk* suppresses the TDP-43-mediated age-dependent neurodegeneration seen in amyotrophic lateral sclerosis (ALS) (Sreedharan et al., 2015). Accumulation of the nuclear RNA-binding protein TDP-43 (encoded by *TARDBP*) in the cytoplasm is the histopathological signature of degenerating neurons in ALS. Investigations of gene expression patterns that accompany TDP-43-induced neurotoxicity in the *Drosophila* system showed the strong upregulation of cell cycle regulators and Notch target genes (Zhan et al., 2013). Mutations in Notch pathway components also

Development (2019) 146, dev170837. doi:10.1242/dev.170837

extended the lifespan of TDP-43 transgenic lines (Zhan et al., 2013). Thus, Notch activation has deleterious effect in TDP-43 flies. Given that the Sreedharan group reported the suppression of TDP-43 toxicity by *htk* mutations, it is tempting to speculate that Htk might also have an important role in the activation of Notch signaling that leads to the TDP-43-mediated neurodegeneration in ALS. If this is the case, then Htk could be considered as a future therapeutic target for ALS.

MATERIALS AND METHODS

Yeast two-hybrid screen

A 393-bp *Drosophila* Notch cDNA (accession number M11664) fragment encoding amino acids 1765-1895 containing NLS was cloned in frame with the sequence encoding the *Lex*A DNA-binding domain of the bait vector. This construct was used as a bait to screen oligo(dT)-primed *D. melanogaster* 0-24 h embryo cDNA libraries cloned in pGAD prey vectors containing GAL4 activation domains. A yeast two-hybrid screen was carried out using a mating approach (Fromont-Racine et al., 1997) with L40ΔGAL4 and Y187 yeast strains. His+ colonies were selected on media lacking tryptophan, leucine and histidine, and all positive pGAD plasmids from His+ colonies were isolated and sequenced to identify interactors (as described by Mukherjee et al., 2005).

Immunoprecipitation and immunoblotting

For co-immunoprecipitation experiments, Notch-ICD was overexpressed in larval salivary glands under the control of a *sgs-GAL4* driver. Salivary glands were dissected and homogenized in lysis buffer [25 Mm Tris (pH 8.0), 27.5 mM NaCl, 20 mM KCl, 25 mM sucrose, 10 mM EDTA, 10 mM EGTA, 1 mM DTT, 10% glycerol, 0.5% Tergitol solution, 1 mM PMSF and 1× protease inhibitor (Roche)]. Crude lysate containing 3 mg of total protein was mixed with 5 µl anti-Htk antibody and 20 µl protein A/G beads and kept on an end-over-end rotator overnight at 4°C. No antibody was added to the control samples. Beads were collected after washing three times with lysis buffer, separated on a 12% denaturing SDS polyacrylamide gel and transferred onto Immuno-Blot PVDF membranes (Bio-Rad). After washing for 10 min in TBST [Tris base (50 mM), NaCl (150 mM) and Tween-20 (0.1%)] followed by blocking (4% skimmed milk in TBST) for 30 min, blots were probed with a mouse anti-Notch antibody [C17.9C6, 1:3000 dilution, Developmental Studies Hybridoma Bank (DSHB)]. After washing again for three times in TBST and blocking (4% skimmed milk in TBST) for 30 min, a goat anti-mouse IgG-AP conjugate (Molecular Probes) diluted at 1:2000 in blocking solution was added for 90 min followed by three washings in TBST. Color was detected by Sigma FAST BCIP/NBT (Sigma).

Similarly, lysates were prepared from larval wing discs expressing Notch-ICD and HA-Htk, and only HA-Htk using a *vg-GAL4* driver, followed by immunoprecipitation with anti-HA affinity beads (Sigma), and anti-Notch antibody along with A/G beads. Monoclonal mouse anti-Notch (C17.9C6) antibodies at a 1:3000 dilution were used to detect Notch; mouse anti-HA antibodies at a 1:1000 dilution (Sigma) were used to detect HA; and rabbit anti-Su(H) antibodies at a 1:1000 dilution (Santa Cruz Biotechnology) was used to detect Su(H). Goat anti-mouse IgG-AP conjugates or anti-rabbit IgG-AP conjugates at a 1:2000 dilution (Molecular Probes) were used as secondary antibodies.

Drosophila genetics

All fly stocks were maintained on standard cornmeal/yeast/molasses/agar medium at 25°C. Oregon-R flies were used as wild-type controls. The *htk*-null mutant alleles, *htk^{71} FRT19A/FM7*, *htk^{39} FRT19A/FM7* and *htk^{47} FRT19A/FM7* were provided by Dr Jemeen Sreedharan, Babraham Institute, Cambridge, UK (Sreedharan et al., 2015). Notch pathway components were provided by Prof. S. Artavanis-Tsakonas, Department of Cell Biology, Harvard Medical School, USA. We used the following stocks for our studies:

For genetic interactions: UAS-dominant-negative Notch (UAS-DNN7)/CyO; C96-GAL4/TM6B, *Su(H)T4/CyO* (gain-of-function allele), *Su(H)1/CyO* (loss-of-function allele) (BL417) and *C96-GAL4*, *UAS-MamH/TM6B* were used.

For epistatic studies: *UAS-Notch-RNAi/CyO* (*UAS-NIRM*), *UAS-Su(H)VP16* (II) (provided by Prof. Sarah Bray, University of Cambridge, UK) and *UAS-Su(H)VP16/TM3 ser* (provided by Prof. Jessica Treisman, School of Medicine, NYU, USA) were used.

For loss- and gain-of-function studies: *UAS-htk-RNAi* (BL31574), *UAS-Notch-RNAi/CyO*, *NRE-eGFP* (BL30728) and *UAS-HA-htk/TM3*, Ser (Fly Line ID: F000657) were used. *UAS-HA-htk* stock (which expresses a functional but truncated form of the Htk protein) was ordered from FlyORF.

GAL4 driver lines: *en-GAL4*, *C96-GAL4*, *Sgs3-GAL4*, *ap-GAL4/CyO*, *MS1096-GAL4*, *vg-GAL4*, *ptc-GAL4*, *ey-GAL4* and *GMR-GAL4* were ordered from the Bloomington *Drosophila* Stock Centre.

For mosaic generation: *hs-FLP neoFRT19A Ubi-RFP* (BL31418) and *neoFRT19A* (BL1709) were used.

To generate somatic clones, we used the FLP/FRT system. Males of the *hs-FLP neoFRT19A Ubi-RFP* strain were crossed with *htk^{71} FRT19A/FM7*, *htk^{47} FRT19A/FM7* and *htk^{39} FRT19A/FM7* females. Heat shock was given at 37°C for 60 min at 24 h after egg laying (AEL), and third-instar female larvae were analyzed for mutant clones. Given that we observed similar phenotypes in all the *htk* alleles, we only show results for the *htk^{71}* mutation.

To generate MARCM-derived clones and *htk^{71}* mutant clones in an *Su(H)VP16* overexpression background, the following flies were generated by appropriate genetic crosses:

hs-FLP neoFRT19A Ubi-RFP/Y; +/+; *C96-GAL4*
hs-FLP neoFRT19A tub-GAL80/Y; +/+; *tub-GAL4 UAS-GFP/TM6c sb*
htk^{71} FRT19A/FM7; UAS-Su(H)VP16
htk^{71} FRT19A/FM7; UAS-NICD
neoFRT19A/FM7; UAS-Su(H)VP16
neoFRT19A/FM7; UAS-NICD

The MARCM system was used to generate GFP-marked *htk^{71}* mutant clones overexpressing either *Notch-ICD* or *Su(H)VP16*. *htk^{71} FRT19A/FM7*; *UAS-Su(H)VP16* and *htk^{71} FRT19A/FM7*; *UAS-NICD* females were crossed to males *hs-FLP neoFRT19A tub-GAL80/Y*; +/+; *tub-GAL4 UAS-GFP/TM6c sb*. In parallel, a control experiment was carried out in which *neoFRT19A/FM7*; *UAS-Su(H)VP16* and *neoFRT19A/FM7*; *UAS-NICD* females were used for crosses. Heat shock was given at 37°C for 60 min at 24 h AEL and third-instar female larvae were analyzed for GFP-marked clones.

To generate *htk^{71}* mutant clones in a *Su(H)VP16* overexpression background, *hs-FLP neoFRT19A Ubi-RFP/Y*; +/+; *C96-GAL4* males were crossed with *htk^{71} FRT19A/FM7*; *UAS-Su(H)VP16* females (experimental) and *neoFRT19A/FM7*; *UAS-Su(H)VP16* females (controls). The remainder of the procedure was as previously detailed.

Eye imprints

Eye imprints using nail polish were made for analyzing ommatidial defects, and were examined under differential interference contrast (DIC) optics on a Nikon Eclipse Ni microscope.

RNA isolation, semiquantitative and RT quantitative PCR

Total RNA was isolated from imaginal discs of third instar larvae using TRIZOL reagent following the manufacturer's recommended protocol (Sigma-Aldrich). RNA (1 µg) was treated with DNAse using 1.0 µl 10× reaction buffer, 0.5 µl DNAse (New England Biolabs) and 0.5 µl RNAse inhibitor (1,000 U/ml), and volume was adjusted to 10 µl using DEPC MilliQ water. The reaction mixture was incubated at 37°C for 1 h, then 1 µl of 25 mM EDTA was added followed by a 10 min incubation at 65°C. For single-stranded cDNA preparation, 10 µl of DNAse-treated RNA was mixed with 1 µl M-MuLV reverse transcriptase enzyme (New England Biolabs), 2 µl of 60 µM random primers, 2 µl of 10× M-MuLV buffer, 1 µl of 10mM dNTP and 1 µl of RNase inhibitor, and nuclease-free water was used to make the total volume to 20 µl. Mix was incubated at 25°C for 5 min followed by a 42°C incubation for 1 h. This cDNA was used as a template DNA for semiquantitative and RT quantitative (RT-q)PCR. RT-qPCR was carried out as per the manufacturer's protocol (Applied Biosystems). A total of 10 µl of the reaction volume included 5 µl 2× SYBR green, 0.25 µl of each forward and reverse primer, and 1 µl cDNA; PCR was performed using an ABI 7500 instrument. Data were normalized to *rps17* before calculating the relative fold change. Primers for RT-qPCR can be found in Table S1.

Development (2019) 146, dev170837. doi:10.1242/dev.170837

Immunostaining of imaginal discs

For immunostaining, imaginal discs from third-instar larvae were dissected in cold PBS, followed by 20-min incubation in 4% paraformaldehyde. Tissues were then washed four times in washing solution [a mixture of 1×PBS, 0.2% Triton-X-100 and 0.1% bovine serum albumin (BSA)] for 10 min each, followed by incubation in blocking solution (Tri-PBS with 0.1% BSA and 8% normal goat serum) for 60 min. Primary antibodies were diluted in blocking solution, added to the ovaries and incubated overnight at 4°C. After four washes in washing solution and 60-min blocking, secondary antibodies were added at a 1:200 dilution and incubated for 90 min at room temperature. This was followed by four washes in washing solution for 15 min each. After a PBS wash, 4′,6-diamidino-2-phenylindole dihydrochloride (DAPI) (1 µg/ml) was added for 20 min to the tissues. After a final dissection in cold PBS, samples were mounted in 1,4-diazabicyclo[2.2.2]octane (DABCO). The following primary antibodies were used: rabbit polyclonal anti-Htk (1:100) (Singh et al., 2018), anti-Notch raised in mouse (1:300) (C17.9C6), mouse anti-Wg (1:100) (4D4), mouse anti-Cut (1:100) (2B10; DSHB), mouse anti-HA (1:100) (Sigma) and mouse anti-βGAL (1.5:100) (Promega). The secondary antibodies used were: Alexa Fluor 555 conjugated goat anti-mouse IgG (1:200), Alexa Fluor 488 conjugated goat anti-mouse IgG (1:200), Alexa Fluor 555 conjugated goat anti-rabbit IgG (1:200), Alexa Fluor 555 conjugated goat anti-rat IgG (1:200) and Alexa Fluor 488 conjugated goat anti-rabbit IgG (1:200) (all from Molecular Probes). Fluorescent images were obtained with a Carl Zeiss LSM780 confocal microscope.

Chromatin immunoprecipitation

In total, 100 heads were dissected from *GMR-GAL4*, *UAS-HA-htk* flies in 1× PBS and fixed in 1% formaldehyde solution at room temperature for 20 min. Incubation for 1 min in 0.125 M glycine solution was performed to stop crosslinking followed by three washes in 1× cold PBS. Then, 400 µl nuclear lysis buffer[1% SDS, 10 mM EDTA, 50 mM Tris-HCl (pH 8) and 1× protease inhibitor] was added and heads were homogenized followed by sonication (QSonica, Q700) (50 cycles, amplitude of 90, pulse on 30 s, pulse off 1 min). After centrifugation at 13,000 rpm (18,000 ***g***) for 10 min at 4°C, supernatants (chromatin samples) were collected and stored at −20°C. DNA was purified from 50 µl of this chromatin sample using the phenol/chloroform method, for which one volume of phenol:chloroform:isoamyl alcohol (25:24:1) was added to the sample and mixed thoroughly, followed by centrifugation at 15,000 ***g*** at 4°C for 10 min. The upper aqueous phase was removed carefully and transferred to a fresh tube. Sample was mixed with one volume of chloroform:isoamyl alcohol (24:1) by centrifugation at 15,000 ***g*** at 4°C for 10 min and the upper aqueous phase collected again. This was followed by DNA precipitation using 3 mM sodium acetate and absolute ethanol, and the fragment size was checked using agarose gel electrophoresis (image not shown). For immunoprecipitation, 200 µl of the chromatin sample was mixed with 25 µl pre-washed HA beads (Sigma) and ChIP dilution buffer [0.01% SDS, 1.1 % Triton X-100, 1.2 mM EDTA, 16.7 mM TrisHCl (pH 8), 167 mM NaCl]. was added to make up the final volume to 300 µl. Mock-IP was used as negative control in which, A/G beads (Santa Cruz Biotechnology) were added instead of HA beads in the chromatin sample. The mixed sample was kept for end-over-end rotation at 4°C overnight. Beads were then washed with a low-salt wash buffer [0.1% SDS, 1% TritonX-100, 2 mM EDTA, 20 mM Tris-HCl (pH 8), 150 mM NaCl], a high-salt wash buffer [0.1% SDS, 1% TritonX-100, 2 mM EDTA, 20 mM Tris-HCl (pH 8), 0.5 M NaCl], LiCl wash buffer [25 mM LiCl, 1% NP-40, 1% NaDOC, 1 mM EDTA, 10 mM Tris-Cl (pH 8)] and TE buffer [10 mM Tris-HCl (pH 8), 1 mM EDTA]. Beads were resuspended in 150 µl ChIP elution buffer (50 mM $NaHCO_3$, 1% SDS) and vortexed gently for 15 min at room temperature, followed by centrifugation at 2000 rpm (425 ***g***) for 4°C; the supernatants were then collected. This step was repeated twice and the samples were pooled; 1 µl of RNase with 18 µl 5 M NaCl was then added and incubated at 67°C for 4-5 h. 25 µl 5× PK buffer [50 mM Tris-HCl (pH 8), 25 mM EDTA.NA_2, 1.25% SDS] and 1.5 µl proteinase K (10 mg/ml) was added and incubated at 45°C for 2 h. Thereafter, the DNA was purified using phenol/chloroform extraction and ethanol precipitation followed by resuspension in 30 µl TE buffer. PCR was performed using 2 µl eluted DNA as a template and the primers are described in Table S2.

Acknowledgements

The authors thank Prof. Spyros Artavanis-Tsakonas (Department of Cell Biology, Harvard Medical School, USA) for Notch pathway mutant *Drosophila* stocks. Prof. Jessica Treisman (School of Medicine, NYU, USA) and Prof. Sarah Bray (University of Cambridge, UK) are acknowledged for *Su(H)VP16* stocks and Dr Jemeen Sreedharan (Babraham Institute, Cambridge, UK) is acknowledged for providing *htk* mutant alleles. The Bloomington *Drosophila* Stock Center is acknowledged for providing fly stocks. We also acknowledge the confocal facility of the Interdisciplinary School of Life Sciences, Banaras Hindu University.

Competing interests

The authors declare no competing or financial interests.

Author contributions

Conceptualization: A.S., A.M.; Methodology: A.S., M.S., P.D.D.; Validation: A.S.; Formal analysis: A.S.; Investigation: A.S., M.M., A.M.; Writing - original draft: A.S., A.M.; Writing - review & editing: A.S., A.M.; Visualization: A.S.; Supervision: A.M.; Project administration: M.M., A.M.; Funding acquisition: M.M., A.M.

Funding

This work was supported by a grant from Department of Biotechnology, Ministry of Science and Technology, Government of India (to A.M. and M.M.). A.S. and D.D. receive fellowship support from the Council of Scientific and Industrial Research, India, and M.S.P. receives fellowship support from a Jawaharlal Nehru Memorial Fund fellowship.

Supplementary information

Supplementary information available online at
http://dev.biologists.org/lookup/doi/10.1242/dev.170837.supplemental

References

Akhtar, A., Zink, D. and Becker, P. B. (2000). Chromodomains are protein-RNA interaction modules. *Nature* **407**, 405-409. doi:10.1038/35030169

Andersson, E. R., Sandberg, R. and Lendahl, U. (2011). Notch signaling: simplicity in design, versatility in function. *Development* **138**, 3593-3612. doi:10.1242/dev.063610

Artavanis-Tsakonas, S., Rand, M. D. and Lake, R. J. (1999). Notch signaling: cell fate control and signal integration in development. *Science* **284**, 770-776. doi:10.1126/science.284.5415.770

Baron, M., Aslam, H., Flasza, M., Fostier, M., Higgs, J. E., Mazaleyrat, S. L. and Wilkin, M. B. (2002). Multiple levels of Notch signal regulation. *Mol. Membr. Biol.* **19**, 27-38. doi:10.1080/09687680110112929

Blaumueller, C. M., Qi, H., Zagouras, P. and Artavanis-Tsakonas, S. (1997). Intracellular cleavage of Notch leads to a heterodimeric receptor on the plasma membrane. *Cell* **90**, 281-291. doi:10.1016/S0092-8674(00)80336-0

Borggrefe, T. and Oswald, F. (2016). Setting the stage for Notch: the *Drosophila* Su(H)-hairless repressor complex. *PLoS Biol.* **14**, 1-8. doi:10.1371/journal.pbio.1002524

Bouazoune, K., Mitterweger, A., Langst, G., Imhof, A., Akhtar, A., Becker, P. B. and Brehm, A. (2002). The dMi-2 chromodomains are DNA binding modules important for ATP-dependent nucleosome mobilization. *EMBO J.* **21**, 2430-2440. doi:10.1093/emboj/21.10.2430

Brand, A. H. and Perrimon, N. (1993). Targeted gene expression as a means of altering cell fates and generating dominant phenotypes. *Development* **118**, 401-415.

Bray, S. and Furriols, M. (2001). Notch pathway: making sense of suppressor of hairless. *Curr. Biol.* **11**, R217-R221. doi:10.1016/S0960-9822(01)00109-9

Brehm, A., Langst, G., Kehle, J., Clapier, C. R., Imhof, A., Eberharter, A., Müller, J. and Becker, P. B. (2000). dMi-2 and ISWI chromatin remodeling factors have distinct nucleosome binding and mobilization properties. *EMBO J.* **19**, 4332-4341. doi:10.1093/emboj/19.16.4332

Brou, C., Logeat, F., Gupta, N., Bessia, C., LeBail, O., Doedens, J. R., Cumano, A., Roux, P., Black, R. A. and Israël, A. (2000). A novel proteolytic cleavage involved in Notch signaling: the role of the disintegrin-metalloprotease TACE. *Mol. Cell.* **5**, 207-216. doi:10.1016/S1097-2765(00)80417-7

Cabrera, C. V. (1990). Lateral inhibition and cell fate during neurogenesis in *Drosophila*: the interactions between scute, Notch and Delta. *Development* **110**, 733-742.

Cao, J., Gao, T., Stanbridge, E. J. and Irie, R. (2001). RBP1L1, a retinoblastoma-binding protein-related gene encoding an antigenic epitope abundantly expressed in human carcinomas and normal testis. *J. Natl. Cancer Inst.* **93**, 1159-1165. doi:10.1093/jnci/93.15.1159

Casso, D. J., Biehs, B. and Kornberg, T. B. (2010). A novel interaction between hedgehog and notch promotes proliferation at the anterior–posterior organizer of the *Drosophila* wing. *Genetics* **187**, 485-499. doi:10.1534/genetics.110.125138

Cau, E. and Blader, P. (2009). Notch activity in the nervous system: to switch or not switch? *Neural Dev.* **4**, 36. doi:10.1186/1749-8104-4-36

de Celis, J. F., de Celis, J., Ligoxygakis, P., Preiss, A., Delidakis, C. and Bray, S. (1996). Functional relationships between Notch, Su(H) and the bHLH genes of the E(spl) complex: the E(spl) genes mediate only a subset of Notch activities during imaginal development. *Development* **122**, 2719-2728.

De Strooper, B., Annaert, W., Cupers, P., Saftig, P., Craessaerts, K., Mumm, J. S., Schroeter, E. H., Schrijvers, V., Wolfe, M. S., Ray, W. J. et al. (1999). A presenilin-1-dependent gamma-secretase-like protease mediates release of Notch intracellular domain. *Nature* **398**, 518-522. doi:10.1038/19083

Defeo-Jones, D., Huang, P. S., Jones, R. E., Haskell, K. M., Vuocolo, G. A., Hanobik, M. G., Huber, H. E. and Oliff, A. (1991). Cloning of cDNAs for cellular proteins that bind to the retinoblastoma gene product. *Nature* **352**, 251-254. doi:10.1038/352251a0

Delidakis, C. and Artavanis-Tsakonas, S. (1992). The Enhancer of split [E(spl)] locus of *Drosophila* encodes seven independent helix-loop-helix proteins. *Proc. Natl. Acad. Sci. USA* **89**, 8731-8735. doi:10.1073/pnas.89.18.8731

Egan, S. E., St-Pierre, B. and Leow, C. C. (1998). Notch receptors, partners and regulators: from conserved domains to powerful functions. *Curr. Top. Microbiol. Immunol.* **228**, 273-324. doi:10.1007/978-3-642-80481-6_11

Fehon, R. G., Johansen, K., Rebay, I. and Artavanis-Tsakonas, S. (2007). Complex cellular and subcellular regulation of notch expression during embryonic and imaginal development of *Drosophila*: implications for notch function. *J. Cell Biol.* **113**, 657-669. doi:10.1083/jcb.113.3.657

Fleischer, T. C., Yun, U. J. and Ayer, D. E. (2003). Identification and characterization of three new components of the mSin3A corepressor complex. *Mol. Cell. Biol.* **23**, 3456-3467. doi:10.1128/MCB.23.10.3456-3467.2003

Fortini, M. E. (2009). Notch signaling: the core pathway and its posttranslational regulation. *Dev. Cell* **16**, 633-647. doi:10.1016/j.devcel.2009.03.010

Fortini, M. E. and Artavanis-Tsakonas, S. (1994). The Suppressor of Hairless protein participates in Notch receptor signaling. *Cell* **79**, 273-282. doi:10.1016/0092-8674(94)90196-1

Fromont-Racine, M.Rain, J. C. and Legrain, P. (1997). Toward a functional analysis of the yeast genome through exhaustive two-hybrid screens. *Nat. Genet.* **16**, 277-282.

Furriols, M. and Bray, S. (2000). Dissecting the mechanisms of Suppressor of Hairless function. *Dev. Biol.* **227**, 520-532. doi:10.1006/dbio.2000.9923

Gaudet, P., Livstone, M. and Thomas, P. (2010). Gene Ontology annotation inferences using phylogenetic trees. GO Reference Genome Project. http://www.geneontology.org/cgi-bin/references.cgi#GO_REF0000033.

Giaimoa, B. D., Oswaldb, F. and Borggrefe, T. (2017). Dynamic chromatin regulation at Notch target genes. *Transcription* **8**, 61-66. doi:10.1080/21541264.2016.1265702

Go, M. J. and Artavanis-Tsakonas, S. (1998). A genetic screen for novel components of the Notch signaling pathway during *Drosophila* bristle development. *Genetics.* **150**, 211-220.

Guruharsha, K. G., Kankel, M. W. and Artavanis-Tsakonas, S. (2012). The Notch signalling system: recent insights into the complexity of a conserved pathway. *Nat. Rev. Genet.* **13**, 654-666. doi:10.1038/nrg3272

Hartenstein, V. and Posakony, J. W. (1990). A dual function of the Notch gene in *Drosophila* sensillum development. *Dev. Biol.* **142**, 13-30. doi:10.1016/0012-1606(90)90147-B

Helms, W., Lee, H., Ammerman, M., Parks, A. L., Muskavitch, M. A. T. and Yedvobnick, B. (1999). Engineered truncations in the *Drosophila* mastermind protein disrupt Notch pathway function. *Dev. Biol.* **215**, 358-374. doi:10.1006/dbio.1999.9477

Herrscher, R. F., Kaplan, M. H., Lelsz, D. L., Das, C., Scheuermann, R. and Tucker, P. W. (1995). The immunoglobulin heavy-chain matrix-associating regions are bound by Bright: a B cell-specific trans-activator that describes a new DNA-binding protein family. *Genes Dev.* **24**, 3067-3082. doi:10.1101/gad.9.24.3067

Iwahara, J. and Clubb, R. T. (1999). Solution structure of the DNA binding domain from Dead ringer, a sequence-specific AT-rich interaction domain (ARID). *The EMBO J.* **18**, 6084-6094. doi:10.1093/emboj/18.21.6084

Iwahara, J., Iwahara, M., Daughdrill, G. W., Ford, J. and Clubb, R. T. (2002). The structure of the Dead ringer-DNA complex reveals how AT-rich interaction domains (ARIDs) recognize DNA. *EMBO J.* **21**, 1197-1209. doi:10.1093/emboj/21.5.1197

Kadosh, D. and Struhl, K. (1998). Histone deacetylase activity of Rpd3 is important for transcriptional repression invivo. *Genes Dev.* **12**, 797-805. doi:10.1101/gad.12.6.797

Kankel, M. W., Hurlbut, G. D., Upadhyay, G., Yajnik, V., Yedvobnick, B. and Artavanis-Tsakonas, S. (2007). Investigating the genetic circuitry of mastermind in *Drosophila*, a notch signal effector. *Genetics* **177**, 2493-2505. doi:10.1534/genetics.107.080994

Kim, J., Daniel, J., Espejo, A., Lake, A., Krishna, M., Xia, L., Zhang, Y. and Bedford, M. T. (2006). Tudor, MBT and chromo domains gauge the degree of lysine methylation. *EMBO Rep.* **7**, 397-403. doi:10.1038/sj.embor.7400625

Lai, A., Marcellus, R. C., Corbeil, H. B. and Branton, P. E. (1999). RBP1 induces growth arrest by repression of E2F-dependent transcription. *Oncogene* **18**, 2091-2100. doi:10.1038/sj.onc.1202520

Lai, A., Kennedy, B. K., Barbie, D. A., Bertos, N. R., Yang, X. J., Theberge, M.-C., Tsai, S.-C., Seto, E., Zhang, Y., Kuzmichev, A. et al. (2001). RBP1 recruits the mSIN3-histone deacetylase complex to the pocket of retinoblastoma tumor suppressor family proteins found in limited discrete regions of the nucleus at growth arrest. *Mol. Cell. Biol.* **21**, 2918-2932. doi:10.1128/MCB.21.8.2918-2932.2001

Lee, T. and Luo, L. (2001). Mosaic analysis with a repressible cell marker (MARCM) for Drosophila neural development. *Trends Neurosci.* **24**, 251-254. doi:10.1016/S0166-2236(00)01791-4

Liu, J., Sato, C., Cerletti, M. and Wagers, A. (2010). Notch signaling in the regulation of stem cell self-renewal and differentiation. *Curr. Top Dev. Biol.* **92**, 367-409. doi:10.1016/S0070-2153(10)92012-7

Logeat, F., Bessia, C., Brou, C., Lebail, O., Jarriault, S., Seidah, N. G. and Israel, A. (1998). The Notch1 receptor is cleaved constitutively by a furin-like convertase. *Proc. Natl. Acad. Sci. USA* **95**, 8108-8112. doi:10.1073/pnas.95.14.8108

Mukherjee, A., Veraksa, A., Bauer, A., Rosse, C., Camonis, J. and Artavanis-Tsakonas, S. (2005). Regulation of Notch signalling by non-visual β-arrestin. *Nat. Cell Biol.* **7**, 1191-1201. doi:10.1038/ncb1327

Mumm, J. S., Schroeter, E. H., Saxena, M. T., Griesemer, A., Tian, X., Pan, D. J., Ray, W. J. and Kopan, R. (2000). A ligand-induced extracellular cleavage regulates gamma-secretase-like proteolytic activation of Notch1. *Mol. Cell* **5**, 197-206. doi:10.1016/S1097-2765(00)80416-5

Neumann, C. J. and Cohen, S. M. (1996). A hierarchy of cross-regulation involving Notch, wingless, vestigial and cut organizes the dorsal/ventral axis of the *Drosophila* wing. *Development* **122**, 3477-3485.

Patsialou, A., Wilsker, D. and Moran, E. (2005). DNA-binding properties of ARID family proteins. *Nucleic Acids Res.* **33**, 66-80. doi:10.1093/nar/gki145

Rebay, I., Fleming, R. J., Fehon, R. G., Cherbas, L., Cherbas, P. and Artavanis-Tsakonas, S. (1991). Specific EGF repeats of Notch mediate interactions with Delta and Serrate: implications for Notch as a multifunctional receptor. *Cell* **67**, 687-699. doi:10.1016/0092-8674(91)90064-6

Sachan, N., Mishra, A. K., Mutsuddi, M. and Mukherjee, A. (2013). The *Drosophila* importin-α3 is required for nuclear import of Notch in vivo and it displays synergistic effects with Notch receptor on cell proliferation. *PLoS ONE* **8**, 2-10. doi:10.1371/journal.pone.0068247

Silverstein, R. A. and Ekwall, K. (2005). Sin3: a flexible regulator of global gene expression and genome stability. *Curr. Genet.* **47**, 1-17. doi:10.1007/s00294-004-0541-5

Singh, A., Dutta, D., Paul, M. S., Verma, D., Mutsuddi, M. and Mukherjee, A. (2018). Pleiotropic functions of the chromodomain-containing protein hat-trick during oogenesis in *Drosophila melanogaster*. *G3* **8**, 1067-1077. doi:10.1534/g3.117.300526

Spain, M. M., Caruso, J. A., Swaminathan, A. and Pile, L. A. (2010). *Drosophila* SIN3 Isoforms interact with distinct proteins and have unique biological functions. *J. Biochem.* **285**, 27457-27467. doi:10.1074/jbc.M110.130245

Sreedharan, J., Neukomm, L. J., Brown, R. H. and Freeman, M. R. (2015). Age-dependent TDP-43-mediated motor neuron degeneration requires GSK3, hat-trick, and xmas-2. *Curr. Biol.* **25**, 2130-2136. doi:10.1016/j.cub.2015.06.045

Struhl, G. and Adachi, A. (1998). Nuclear access and action of Notch in vivo. *Cell* **93**, 649-660. doi:10.1016/S0092-8674(00)81193-9

Struhl, G. and Greenwald, I. (1999). Presenilin is required for activity and nuclear access of Notch in *Drosophila*. *Nature* **398**, 522-525. doi:10.1038/19091

Suryadinata, R., Sadowski, M., Steel, R. and Sarcevic, B. (2011). Cyclin-dependent kinase-mediated phosphorylation of RBP1 and pRb promotes their dissociation to mediate release of the SAP30 mSin3 HDAC transcriptional repressor complex. *J. Biol. Chem.* **286**, 5108-5118. doi:10.1074/jbc.M110.198473

Wan, C., Borgeson, B., Phanse, S., Tu, F., Drew, K., Clark, G., Xiong, X., Kagan, O., Kwan, J., Bezginov, A. et al. (2015). Panorama of ancient metazoan macromolecular complexes. *Nature* **17**, 339-344. doi:10.1038/nature14877

Wang, Z., Lyu, J., Fang, W., Miao, C., Nan, Z., Zhang, J., Xi, Y., Zhou, Q., Yang, X. and Ge1, W. (2018). The histone deacetylase HDAC1 positively regulates Notch signaling during *Drosophila* wing development. *Biol. Open* **15**, bio029637. doi:10.1242/bio.029637

Wu, L., Aster, J. C., Blacklow, S. C., Lake, R., Artavanis-Tsakonas, S. and Griffin, J. D. (2000). MAML1, a human homologue of *Drosophila* mastermind, is a transcriptional co-activator for NOTCH receptors. *Nat. Genet.* **26**, 484-489. doi:10.1038/82644

Xu, T. and Rubin, G. M. (1993). Analysis of genetic mosaics in developing and adult *Drosophila* tissues. *Development* **117**, 1223-1237.

Ye, Y., Lukinova, N. and Fortini, M. E. (1999). Neurogenic phenotypes and altered Notch processing in *Drosophila* Presenilin mutants. *Nature* **398**, 525-529. doi:10.1038/19096

Zhan, L., Hanson, K. A., Kim, S. H., Tare, T. and Tibbetts, R. S. (2013). Identification of genetic modifiers of TDP-43 neurotoxicity in *Drosophila*. *PLoS ONE* **8**, e57214. doi:10.1371/journal.pone.0057214

Zhou, S., Fujimuro, M., Hsieh, J. J.-D., Chen, L., Miyamoto, A., Weinmaster, G. and Hayward, S. D. (2000). SKIP, a CBF1-associated protein, interacts with the ankyrin repeat domain of NotchIC to facilitate NotchIC function. *Mol. Cell. Biol.* **20**, 2400-2410. doi:10.1128/MCB.20.7.2400-2410.2000

A

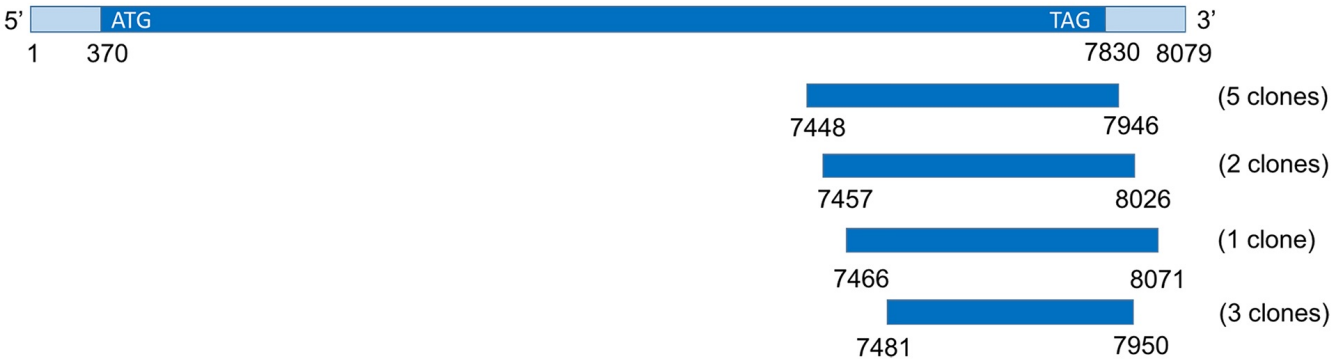

B

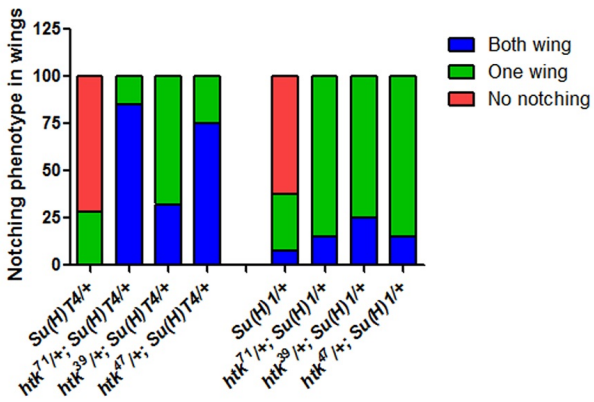

C

Genotype	Phenotypes (%)
+/+; ap-GAL4/+; UAS-htk-RNAi/+	Extra vein material near 2nd Cross Vein : 46% Defect in 2nd cross vein : 60% Extra row of bristles near wing margin : 34% 1st vein defective : 100% Patch of disorganized tissue at the tip of the vein : 60% Blisters in wing : 14% wings directed outward and upward : 100% Increased scutellar bristles : 72%
+/+; MS1096 –GAL4/+; UAS-htk-RNAi/+	Extra row of bristles near wing margin : 89% Patch of disorganized tissue at the tip of the vein : 72% Defect in 1st cross vein : 52%
+/+; +/+; C96 -GAL4 /UAS-htk-RNAi	Defect in 1st cross vein : 44% Extra vein : 12% Unusual bristle pattern : 39% Patch of disorganized tissue at the tip of the vein : 39%
+/+; ptc-GAL4 /+;UAS-htk-RNAi/+	Defect in 1st cross vein : 75% Patch of disorganized tissue at the tip of the vein : 52.5% Extra vein material near cross vein : 13% 1st cross vein very short and reduced intervein distance between L3-L4 : 100%
+/+; +/+; dpp-Gal4/UAS-htk-RNAi	Extra vein material near 2nd cross vein : 7.14% Patch of disorganized tissue at the tip of the vein : 49% Double 1st cross vein : 4%
+/+; en-GAL4/+; UAS-htk-RNAi	mis-oriented bristles and thinner wing blade in posterior region of wings : 75%
+/+; ey-GAL4/+; UAS-htk-RNAi	Reduced eye size :100%

D

Genotype	Phenotypes (100%)
+/+; ap-GAL4/+; UAS-HA-htk/+	• loss of scutellar bristles • reduced size of scutellum • severe wing blisters
+/+; en-GAL4 /+; UAS-HA-htk/+	• bending of third wing vein • thinner wing blade • incomplete fifth vein
+/+; ey-GAL4 /+;UAS-HA-htk/+	• loss of ommatidia
+/+; +/+; GMR-Gal4/UAS-HA-htk	• eye roughening

Figure S1: (A) Schematic representation of the sequence range of 11 positive yeast two-hybrid clones which overlapped with *htk* cDNA, when amino terminus of Notch-ICD (amino acids 1765–1895) was used as bait to screen 6x10^6 cDNAs from a *Drosophila* 0–24 h embryonic library. **(B)** Graph showing the frequency (number) of wing notching phenotypes observed in *Su(H)T4* and *Su(H)1* alleles individually and in trans-heterozygous combination with different *htk* alleles: *htk^{71}, htk^{39}, htk^{47}*. **(C)** Development defects induced by down-regulation of *htk* with a variety of GAL4 drivers, n=200. **(D)** Defects observed in wing and eye when ectopic expression of HA-*htk* was induced with a variety of GAL4 drivers, n=200. All phenotypes examined were 100% penetrant.

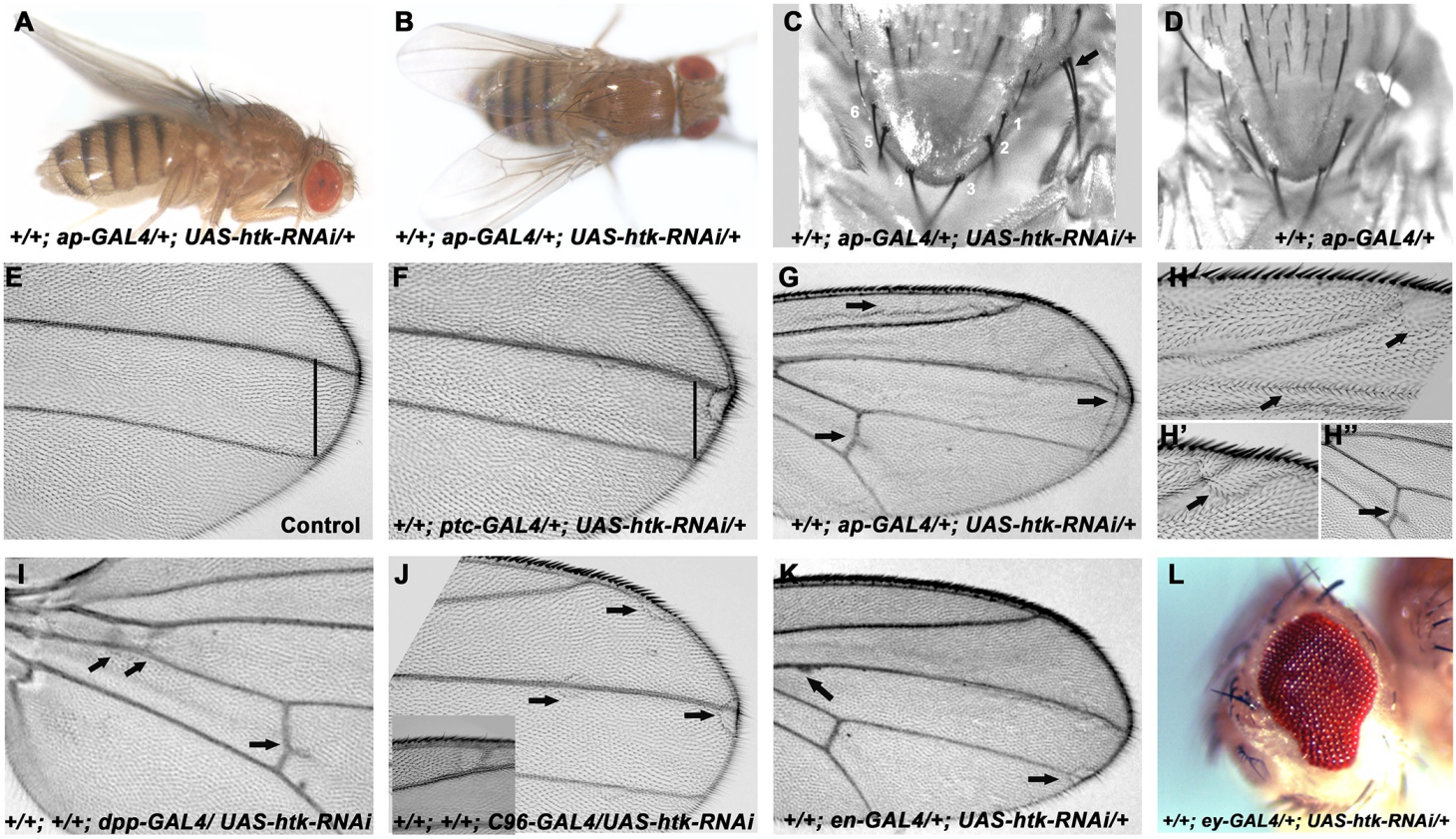

Figure S2: **Down-regulation of *htk* exhibits distinct phenotypes in *Drosophila* wings and eyes. (A-D, G)** *apterous-GAL4* driven *htk-RNAi* displayed upward (A) and outward (B) directed wings with extra rows of sensory bristles and vein material (arrow) in the wingblade (G), and increased scutellar bristles (C) compared to control (D). Similarly when *htk* was down-regulated at anterior-posterior boundary using *patched-GAL4* **(F)** and *dpp-GAL4* **(I),** at wing margin using using *C96-GAL4* **(J)**, in posterior compartment of wing using *engrailed-GAL4* **(K)**, and in the eye using *eyeless-GAL4* **(L)**, it resulted in reduced distance between L3 and L4 veins (black line) **(F)**, extra vein material (arrows) **(I)**, areas with thinner cuticle (arrows) **(J, K)** and reduced eye-size **(L)**, respectively. **(E)** Control adult wing displaying normal wing margin and longitudinal veins L1–L5. **(H-H")** High magnification images of wing showing extra row of bristles (H), area with thinner cuticle (H'), and extra vein material (H''). Several htk down-regulation phenotypes mimic Notch loss-of-function phenotypes.

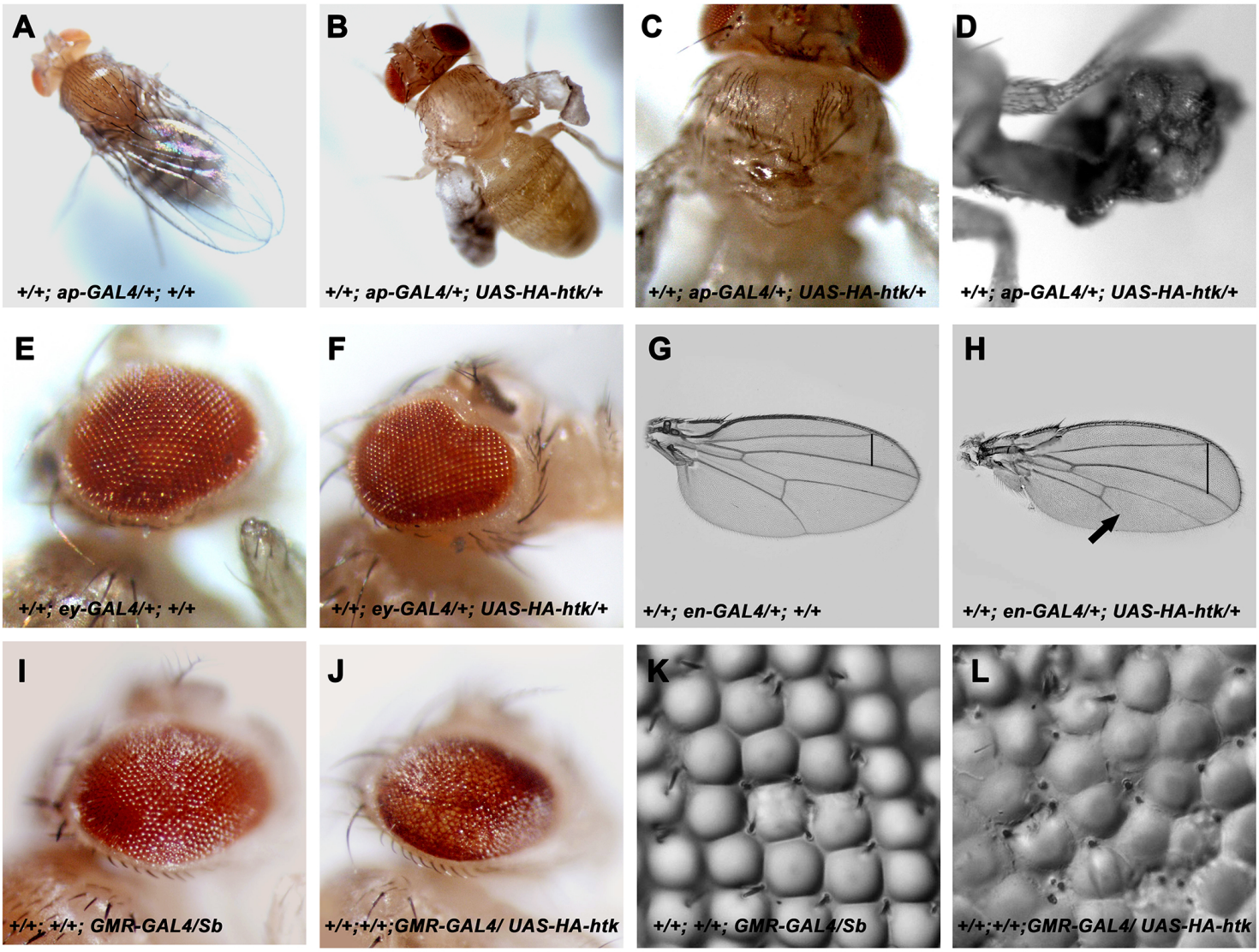

Figure S3: **Over-expression of *htk* resembles *Notch* gain-of-function phenotypes. (A-D)** Ectopic expression of *htk* driven by *apterous-GAL4* causes loss of scutellar bristles **(B, C)** and deformed wing **(B, D)** in comparison to only *apterous-Gal4/+* fly **(A)**. **(E,F)** *eyeless-GAL4* driven expression of *htk* in eye results in loss of ommatidia. **(G,H)** Over-expression of *htk* in posterior region of wing using *engrailed-GAL4* results in incomplete fifth vein and increased inter-vein distance between second and third vein. **(I, J)** Ectopic expression in adult eye using *GMR-GAL4* results in increased eye-roughening and loss of ommatidial bristles. **(K, L)** Nail polish imprint images of adult eye showing these eye phenotypes more clearly. Phenotypes showed 100% penetrance.

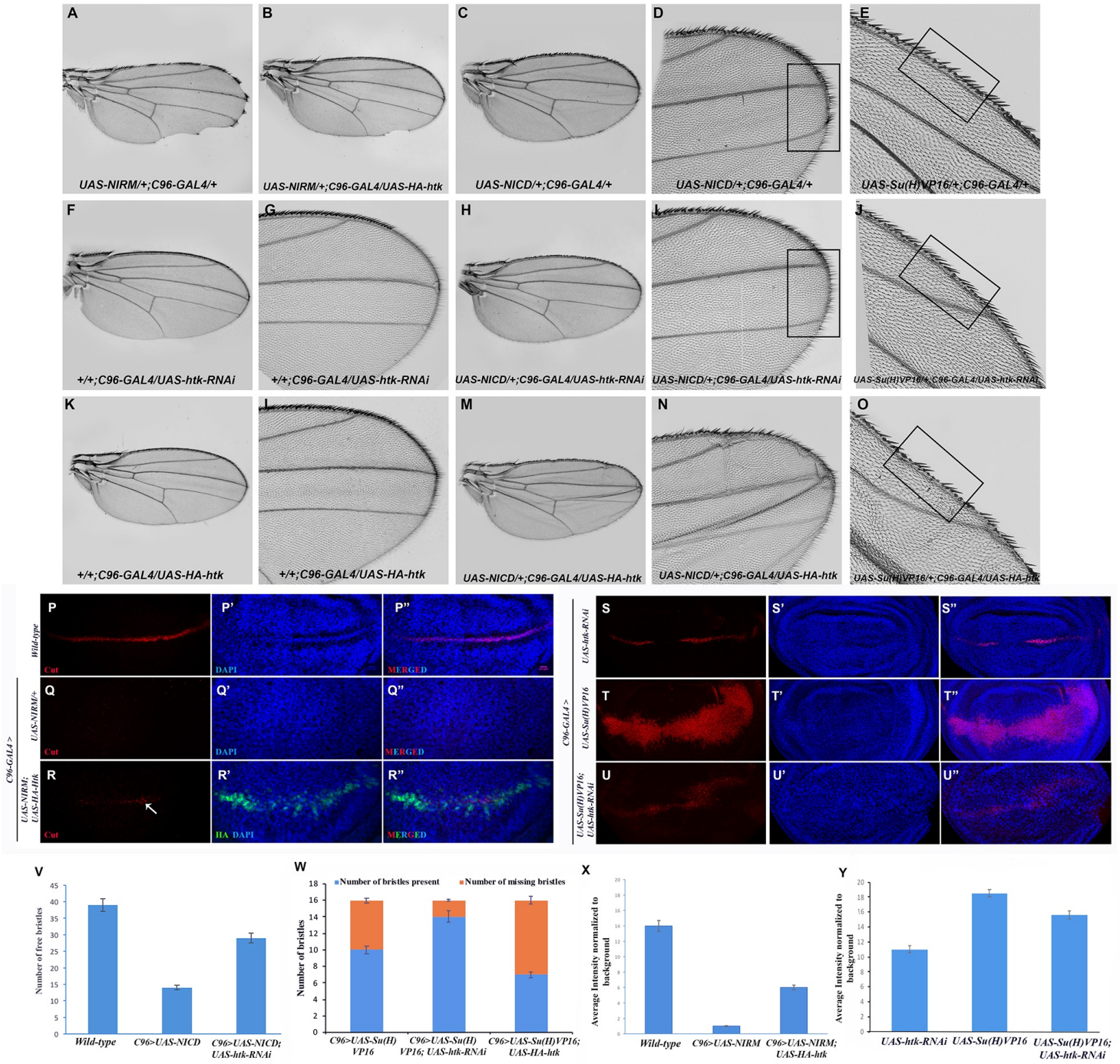

Figure S4: Epistatic interactions of *htk* with Notch pathway. *C96-GAL4* was used to drive the expression of different *UAS* lines at wing margin. **(A-O) Wing images showing epistatic and synergistic interactions between *htk* and *Notch* or *Su(H)VP16***. No notching or bristle irregularities were observed when *htk* was downregulated (F, G), or upregulated (K, L) at the wing margin. When the dose of *htk* was increased in *Notch* loss-of-function background, the wing notching phenotype caused by *Notch-RNAi* (A) was significantly rescued (B). Over-expression of *Notch* (C, D) and *Su(H)VP16* (E) at the wing margin resulted irregularities in wing bristle. This irregularity in bristle pattern was rescued when dosage of *htk* was reduced in this background (H-J). The irregularity in bristle localization was quantified by counting the number of free bristles in the same selected area of wing (n=10) expressing *Notch-ICD* alone and *Notch-ICD* along with *htk-RNAi* (boxed regions, 350µm length) **(V)**, and by counting the number of thick dorsal bristles present or absent in the same selected area of wing expressing *Su(H)VP16* alone and *Su(H)VP16* along with *htk-RNAi* (boxed region, 200µm length) **(W) [**error bars indicate standard error of the mean (n=3)]. The quantification is represented as the graph. Additionally, when *htk* along with *Notch* or *Su(H)VP16* were co-expressed, an increase in the wing margin irregularities was observed (M-O). All the phenotypes showed 100% penetrance (n=100). **(P-U'') Activity of Notch signaling was observed during epistatic interaction of *htk* with *Notch* and *Su(H)VP16***. Notch downstream marker, Cut was used to report the Notch signaling activity. DAPI marked the nuclei. The wild type Cut expression (P) was lost when Notch was reduced at dorso-ventral boundary of wing disc (Q). A rescue in the Cut expression was observed when *HA-htk* was over-expressed in the same background (R). (S-U'') Alternatively, ectopic expression of Cut caused by over-expression of *Su(H)VP16* (T) was partially rescued when *htk* was reduced in this background (U). Images in third column in both the panel are merged of images from first and second column. **(X, Y)** Quantification of Cut signal intensity at dorso-ventral boundary of wing disc is represented in the form of a graph. Cut signals are normalized to background signals, and values relative to controls are presented. Error bars indicate standard error of the mean (n=3). Figure D, G, I, L, N are higher magnification images of C, F, H, K, M, respectively. Scale bar, (P-U'') 10µm.

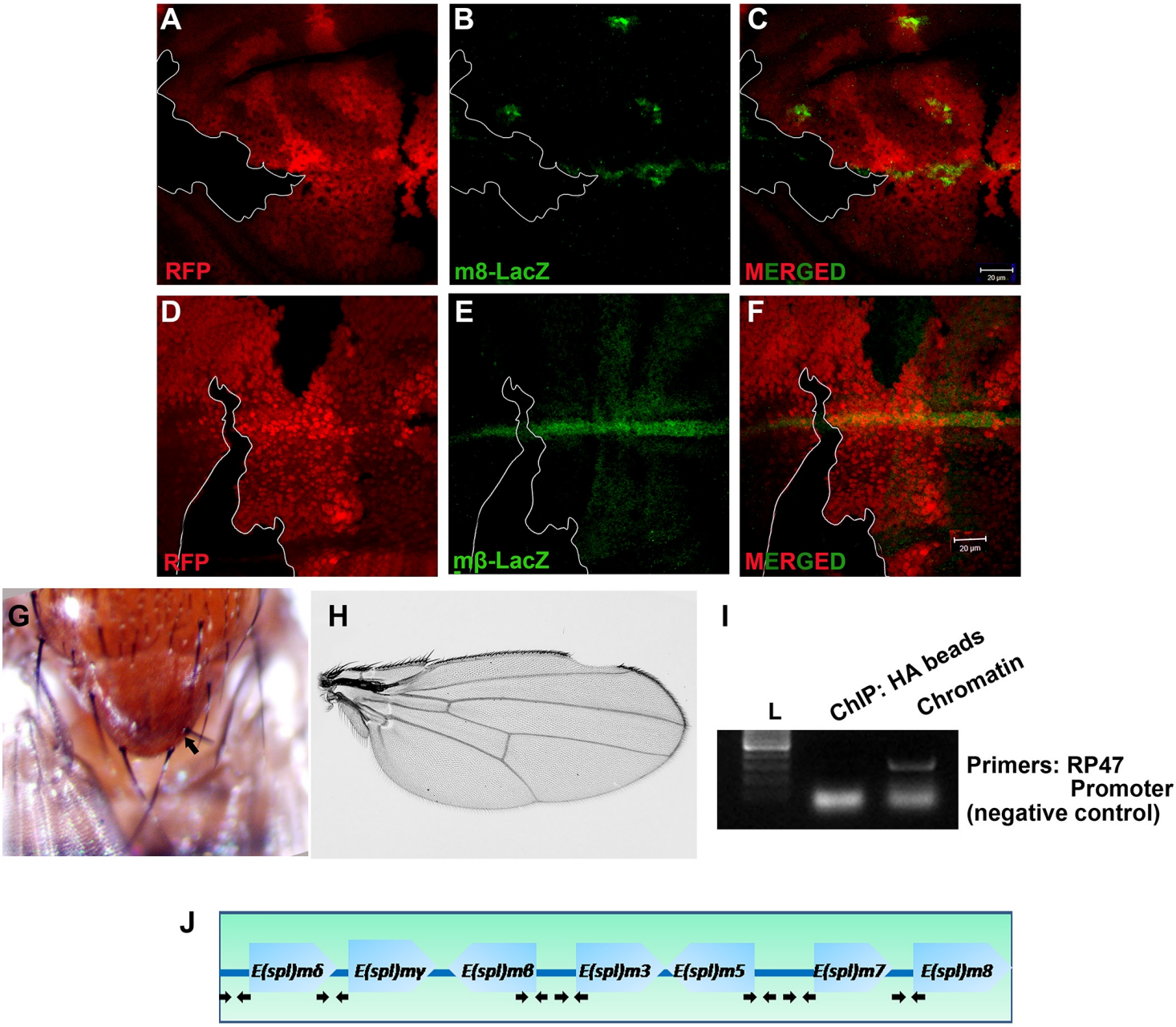

Figure S5: *htk* regulates Notch signaling activity. (A-F) Loss-of-function clones of *htk* displayed reduced expression of *E(spl)* complex genes. **(A, D)** *htk* mutant somatic clones were marked by absence of RFP expression. **(B, E)** The LacZ reporter stocks were used to verify *E(spl)m8* and *E(spl)mβ* expression (shown in green)**.** Third column images are merges of those in first and second columns. The expression of Notch downstream targets, *E(spl)m8* **(A-C)** and *E(spl)mβ* **(D-F)** was significantly reduced in *htk* loss-of-function clones. Scale bar, 20 µM. **(G-H)** Adults developed from larvae containing *htk* loss-of-function somatic clones, displayed various developmental defects such as increased scutellar bristles **(arrow, G),** notching at wing margin **(H),** etc. These phenotypes are also Notch loss-of-function phenotypes. **I.** Agarose gel electrophoresis image for negative control showing that Htk could not immunoprecipitate promoter of *RPS 49* gene. PCR using primers specific for promoter of *RPS 49* gene shows no positive amplification from template DNA fragments which was immunoprecipitated with Htk protein (Lane2). Chromatin samples before immunoprecipitation contain all the genomic DNA fragments, and were used for positive control (Lane 3). **J.** Schematic picture representing the localization of the primers used for ChIP experiment.

Table S1. Primers for RT-qPCR

mβ_RT_Fw 5'- ACCGCAAGGTGATGAAGC -3'
mβ_RT_Re 5'- CTTCATGTGCTCCACGGTC -3'
mδ_RT_Fw 5'- ATGGCCGTTCAGGGTCAG -3'
mδ_RT_Re 5'- CCATGGTGTCCACGATG -3'
mγ_RT_Fw 5'- GTCCGAGATGTCCAAGAC -3'
mγ_RT_Re 5'- GACTCCAAGGTGGCAACC -3'
m3_RT_Fw 5'- ATGGTCATGGAGATGTCC -3'
m3_RT_Re 5'- GCACTCCACCATCAGATC -3'
m5_RT_Fw 5'- ATGGCACCACAGAGCAAC-3'
m5_RT_Re 5'-TGTCCATTCGCAGGATGG -3'
m7_RT_Fw 5'- GGCCACCAAATACGAGATG -3'
m7_RT_Re 5'- CAT CGC CAG TCT GAG CAA -3'
m8_RT_Fw 5'- GGAATACACCACCAAGACC -3'
m8_RT_Re 5'- CGCTGACTCGAGCATCTC -3'

Table S2. Primers for promoter regions

m3_Fw 5’-GATCCAATCCGAAAGCCG-3’
m3_Re 5’-CTAGTTCCCAGCCCTACT-3’
m5_Fw 5’-GTGGTTGTCTGTGTGGAG-3’
m5_Re 5’-GACCTGCTACCTGCGAACA-3’
m7_Fw 5’-GCACGCATGTTCCGTTTG-3’
m7_Re 5’-GGGAAACACTTTGCCCTC-3’
m8_Fw 5’-GCCAATATGCCACATCCAC-3’
m8_Re 5’-GGAACAGCTGCAACTTCG-3’
mβ_Fw 5’-ACTTCGATCGGTTCCCAG-3’
mβ_Re 5’-GAACTGGACAGTGAGTGC-3’
mδ_Fw 5’-GCGGCACAATCCCAATAC-3’
mδ_Re 5’-CTGGTTCCCACTTCCCT-3’
mγ_Fw 5’-CACTCCGTTTACAAATCCCTG-3’
mγ_Re 5’-GCTAGACCTTCGGTGATC-3’